REVIEW 1: Stefano Tavani (University of Naples)				
Point No.		**Comment of the referee** (line numbers refer to the initial version of the manuscript)	**Response of the authors**	**Implemented changes** (line numbers refer to the annotated version of the revised manuscript)
Technical comments	**1**	**page 2 line 25**: "only" = to be omitted	The word "only" will be removed.	Changes made in line 29
	2	**page 2 line 26-27:** linking sentence between two paragraphs is missing	We will change the last two paragraphs of the 'Introduction' chapter in the revised manuscript as follows: "The focus of this work is an in-depth analysis of deformation structures in the southernmost part of a typical foreland basin system, the German Molasse Basin. A number of basin-scale structural studies were carried out in the '80s and '90s, based on a large amount of 2D seismic data acquired for hydrocarbon exploration over decades (e.g. Bachmann et al., 1982; Bachmann et al., 1987; Müller et al., 1988; Bachmann and Müller, 1992). The increasing interest in geothermal exploitation in recent years and therefore the acquisition of 3D seismic data, have allowed more detailed studies of the complexly deformed areas (e.g. Lüschen et al., 2011; von Hartmann et al., 2016; Budach et al., 2017). Nevertheless, the tectonic and stratigraphic factors controlling the evolution of the deformation structures in the German Molasse Basin have not been fully described yet. Using the 3D seismic reflection data, acquired in the area of Geretsried, 30 km south of Munich (Fig. 1), our aim is to understand the complex structure and tectonic evolution of an area proximal to the Alpine deformation front. To achieve this, we analyse the seismic data to (i) reconstruct the temporal and spatial evolution of the fault network within the Molasse sequence and its Mesozoic substratum, and (ii) evaluate the impact of the evolving stress field, pre-existing deformation structures, and mechanical stratigraphy on fault evolution, in particular style of faulting and kinematic interactions between faults."	Changes made in lines 31-45
	3	**page 2 line 44:** "proximal" = to be omitted	The word "proximal" will be removed.	Changes made in line 56
	4	**page 2 line 45:** "by the Tethys Ocean" = to be omitted	The phrase "by the Tethys Ocean" will be removed.	Changes made in lines 56-57
	5	**page 3 line 68:** "terrestrial" to be replaced with "continental"	We will correct the manuscript accordingly.	Changes made in line 110
	6	**page 6 line 159:** "that" = to be replaced with "and"	We will rewrite this sentence as follows: "Unit 1 corresponds to the Upper Jurassic carbonate platform that has a heterogeneous, low-frequency seismic expression."	Changes made in lines 204-205
	7	**page 7 line 199:** terms "synthetic" and "antithetic" faults are misleading	We will remove these terms from the manuscript.	Changes made in lines 245-246

Technical comments	8	**page 7 line 201:** listric geometry of Fault Gartenberg N is not convincing	We agree with the referee that due to the poor resolution at the depth of the investigated graben-bounding faults Gartenberg S and Gartenberg N, especially at the interval of top Callovian, their interpretation as listric could be not fully convincing. We will therefore refrain from this interpretation in the revised version of the manuscript.	Changes made in line 247
	9	**page 7 line 211**: "and secondary, antithetic" = to be omitted	See point 7.	Changes made in line 258
	10	**page 7 line 211: "**...the central graden switches its polarity along strike…"	We will change the text in accordance with the suggestion of the referee.	Changes made in lines 258-259
	11	**page 8 line 215-216:** "there is a rollover anticline towards Fault Gartenberg N" = It is hard to see this rollover anticline, particularly at the top Callovian. Suggest to remove this sentence.	We agree with the referee that interpretation of the central graben interior as a rollover structure could be ambiguous. We therefore refrain from this interpretation and we will remove this sentence as suggested by the referee.	Changes made in lines 260-265
	12	**page 8 line 220-222:** "The upper fault array exhibits reverse/normal fault geometry"	We will change the text accordingly.	Changes made in lines 267
	13	**page 8 line 222-223:** "lateral offset" = strike-slip faults? Clarification needed.	We will change the sentence to clarify what was initially meant by the "lateral offset" as follows: "In the map view the traces of the upper faults at top Rupelian show considerable offset from the traces of the lower faults at top Berriasian" Also, in line 311 we will change the term "lateral offset" to "fault trace offset".	Changes made in lines 270-271 and line 373
	14	**page 8 line 223:** Fig. 12 was called 10 and 11 before	Fig. 12 shows the map view of the fault traces of both fault arrays at different stratigraphic levels to depict the fault trace offset between the faults and compare strike directions.	No changes made to the text
	15	**page 8 line 225:** "often showing opposing dip with respect to each other" = unclear/repetition	We will remove this part of the sentence.	Changes made in lines 273-274
	16	**page 8 line 234:** "Its upper branch dips parallel to the lower thrust within…"	We will change the text accordingly.	Changes made in lines 283
	17	**page 8 line 246:** "cuts over the linkage zone"	We will change this as follows: "cuts through the linkage zone".	Changes made in lines 296-297
	18	**page 8 line 247:** "the Geretsried Fold is extensively deformed by back-thrusts …" - The reviewer recognizes only one back-thrust.	Back-thrusts presented in Figs. 4 and 6 are separate faults. We therefore use the plural. We will remove the word "extensively".	Changes made in lines 297-298
	19	**page 9 line 256-257:** "Unit 1 in Figure 14a displays no significant thickness variation across major faults that offset basement" = Mention that thinning of this unit in the Gartenberg graben is a geometric artifact, due to the fact that the conjugate faults bounding the graben intersect within this unit.	We will change the text to point out thickness reduction of Unit 1 within the central "Gartenberg" graben as follows: "Unit 1 displays substantial thinning within the central graben" However, we believe that this thickness reduction is not a geometric artefact but rather a true geological feature. To explain this, we initially came up with the interpretation of listric graben-bounding faults that propagate into a detachment that accommodates flexure-induced extension. Such interpretation would resolve the geometric space problem associated with the thinning of Unit 1 in the absence of significant offset on graben-bounding faults at top Callovian. As mentioned in point 8, we now refrain from this interpretation and suggest an alternative scenario to explain the thinning of the graben interior. In the revised text we will suggest that this thinning could result from the sequential slip of conjugate faults Gartenberg N and Gartenberg S that offset each other (e.g., Ferrill et al., 2000, 2009).	Changes made in lines 311-314

Technical comments	20	**page 9 line 258-260:** 'There are however local thickness variations in form of footwall thinning and hanging-wall thickening across Fault Gartenberg S, eastern segment of Fault NE and Fault Gartenberg N, and the central segment of Fault Gelting N.' = Remark that these are due to local tilting (i.e. you are considering the vertical thickness not the true one).	The local tilting of the beds indeed results in apparent thickening in the isochore maps. However, apart from the apparent thickening, which is related to tilting, we also observe true local thinning in the footwalls that we attribute in the "Discussion" chapter to the ductile deformation of the clays.	No changes made to the text
	21	**page 9 line 265-266:** 'In the southern part, there is a profound thickness decrease of Unit 4 associated with downthrow of the hanging-wall blocks of the upper CZ normal faults' - modify sentence as follows: 'In the southern part, there is a profound thickness decrease of Unit 4 associated with downthrow of the hanging-wall blocks of the upper CZ normal faults (affecting the overlying Unit 5), which induced compaction in Unit 4.'	We will change the text as follows: 'In the southern part, there is a profound thickness decrease of Unit 4 associated with downthrow of the hanging-wall blocks of the upper CZ normal faults affecting the overlying Unit 5.' We believe that the thickness reduction is primary due to the listric geometry of the CZ faults as we point out in the 'Discussion' chapter.	Changes made in lines 324-325
	22	**page 10 line 284:** "An Allan map of the Geretsried Thrust depicts the distribution of its throw at top Baustein beds" instead of "A map of the cut-off lines at top Baustein beds depicts the lateral distribution of throw on the Geretsried Thrust"	We will change the text in accordance with the suggestion of the reviewer.	Changes made in lines 344-345
	23	**page 11 line 324:** "6.2. Controlling factors on fault evolution in the southern GMB" - suggest to remove this to avoid 4 levels of subheading, i.e. stress field evolution = 6.2; pre-existing structures = 6.3; Pre-orogenic...=6.3.1	We will change the numeration of the subheadings in accordance with the suggestion of the referee.	Changes made to the subheadings of the manuscript
	24	**page 11 line 338:** "eventually increased" instead of "attained positive values"	We will change the text in accordance with the suggestion of the referee.	Changes made in lines 408-411
	25	**page 14 line 435:** the occurance of the rollover structures is not convincing	We agree. See points 8 and 19. We will change the text accordingly.	Changes made in lines 539-543
	26	**page 15 line 466:** "thereby switching from being blind to syn-sedimentary" = to be removed on the ground that a blind fault can be syn-sedimentary	We agree with the point of the referee that the blind faults can also be syn-sedimentary. We will write: "thereby switching from being blind to emergent."	Changes made in line 577

Technical comments	**27**	**page 16 line 486-487:** "We conclude that the fault evolution in the presence of a thick mechanical barrier resulted in a decoupled structural style" = A few readings that could help in framing this last sentence in a broader context: D.A. Ferrill, A.P. Morris, K.J. Smart Stratigraphic control on Extensional fault propagation folding: Big Brushy Canyon monocline, Sierra del Carmen, Texas Geol. Soc. Lond. Spec. Pub., 292 (2007), pp. 203-217 M.M. Lewis, C.A.L. Jackson, R.L. Gawthorpe Salt-influenced normal fault growth and forced folding: the Stavanger fault system, North Sea J. Struct. Geol., 54 (2013), pp. 156-173 J. Deckers Decoupled extensional faulting and forced folding in the southern part of the Roer Valley Graben, Belgium J. Struct. Geol., 81 (2015), pp. 125-134	We will rewrite the sentence as follows: "We conclude that the fault evolution in the presence of a thick mechanical barrier resulted in a decoupled structural style, as has been previously reported for the geometrically decoupled fault systems by Ferrill et al. (2007), Langhi et al. (2011), Lewis et al. (2013), and Deckers (2015)."	Changes made in lines 600-601
Figures	**28**	Figure 2 could be placed within Figure 1	We will place the cross-section in Figure 2 as a panel in Figure 1.	Figure 2 is placed within Figure 1 as panel 1c
	29	Figures 9 and 13 are useless and could be removed.	We will remove these figures in the revised manuscript and modify the text accordingly.	Figs. 9 and 13 are removed
	30	Figure 4, 5, and 6 could be easily merged into a single figure.	Seismic cross-sections in these figures will be placed as panels in a single figure.	Figs. 4, 5, and 6 are Figs. 3a, b, c in the revised manuscript
	31	Figure 10 and 11 could be merged.	We will merge them.	Figs. 10 and 11 are Figs. 5a and b in the revised manuscript
	32	Figures 8 and 12 should be merged and displayed after figures 10 and 11. Figure 19 should be presented as a plate of figure 8.	We will do that.	Figs. 8, 12, and 19 are Figs. 6a-f, h, and g, respectively, in the revised manuscript
	33	Figures 15, 16 and 17 could be merged into a single figure.	We will merge these figures into a single figure.	Figs. 15, 16, and 17 are Figs. 8a, b, and c in the revised manuscript

REVIEW 2: Hugo Ortner (University of Innsbruck)				
Point No.		**Comment of the referee** (line numbers refer to the initial version of the manuscript)	**Response of the authors**	**Implemented changes** (line numbers refer to the annotated version of the revised manuscript)
Specific comments	**1**	**page 2 line 49-50:** 'the authors describe the unconformity at the base of the foreland succession as a result of "…the Late Cretaceous-Paleocene contractional event as consequence of the change in the African plate motion…". However, in most publications on the Alpine Foreland Basin, this unconformity is referred to as the "foreland unconformity", which has been described as a result of the passage of the forebulge rolling through. In their figure 3, the authors label the unconformity as the foreland unconformity. This should be discussed in this paragraph.	We thank the referee for noticing a very important point on the origin of the foreland unconformity. We admit that in our description of the geological setting and in the further interpretation of the faulting phases, we overlook the forebulge hypothesis that was first expressed by Allen et al. (1991), concerning the formation of the basal unconformity of the Molasse Basin. The documented features of this unconformity, such as the NW-directed truncation of the Mesozoic and the progressive onlap of the syn-orogenic deposits onto the peneplained Mesozoic rocks, directed roughly parallel to the Alpine front (Lemcke, 1988, Freudenberger & Schwerd, 1996), clearly points to the forebulge erosion. Allen et al. (1991) puts a temporal constraint on the initial forebulge uplift to the Pliocene times, based on the age of the flysch sediments that conformably overlay the Mesozoic basement in the Ultrahelvetic realm. It has also been recognized that the Mesozoic rocks had been partially and presumably locally truncated, prior to the Pliocene times, during the Sanonian compressional deformation (Lemcke, 1981; Ziegler, 1990; Bachmann and Müller, 1991; Roeder and Bachmann, 1996). Ziegler (1987, 1990) associates this compressional deformation with the initiation of the Alpine thrusting. However, Kley and Voigt (2015) argue for a Late Cretaceous contractional pulse, characterized by the NNE—SSW-oriented thrusting, which is the result of the change in Africa's motion relative to Europe from the SSE-directed sinistral transform motion to the NE-directed convergence. Considering these interpretations, we can thus conclude that the basal foreland unconformity represents a composite hiatus due to the Late Cretaceous basin inversion (unrelated to the early Alpine orogeny) and the Palaeogene passage of the forebulge. The corresponding paragraph in the "Geological Setting" chapter will therefore be modified accordingly as follows: "The sedimentation of the Mesozoic passive margin terminated with the onset of Late Cretaceous compressional deformation. It is widely accepted to have been caused by the inception of the NW-directed Alpine thrusting (Ziegler, 1987, 1990). However, Kley and Voigt (2015) argue that the Late Cretaceous pulse of the NNE—SSW-oriented contraction reflects the change of Africa's motion relative to Europe from south-easterly to north-easterly. As the result of the Late Cretaceous intraplate contraction, the Mesozoic passive margin was subjected to localized inversion and erosion (Bachmann and Müller, 1991; Roeder and Bachmann, 1996). Throught the Palaeocene to Middle Eocene the Alpine foreland was exposed to widespread erosion (Lemcke, 1981) due to the migration of the flexural forebulge in advance of the Alpine orogen (Allen et al., 1991). Subsequent flexural subsidence in the GMB began in the Late Eocene, marking the onset of foredeep sedimentation. As the Alpine orogen continued to move forward, the basin fill progressively onlapped in NW-direction onto the truncated Mesozoic basement and locally, Palaeozoic rocks (Lemcke, 1988, Freudenberger & Schwerd, 1996), forming an angular basal foreland unconformity, referred to as the forebulge unconformity by Allen et al. (1991)."	Changes made in lines 63-75

Specific comments	2	**page 11 lines 329-339:** In their discussion of stress field evolution, the authors claim that the lower normal fault array formed when the forebulge reached the study area. However, the forebulge should have passed the area already when the foreland unconformity formed. At any stage of the foreland basin, the forebulge should be positioned north of the pinchout of any wedge-shaped sedimentary body onlapping the forebulge. Lemcke (1988), and more recently Freudenberger & Schwerd (1996) published maps displaying pinchout-lines of most units of the foreland basin fill. These data should be respected, or it should be discussed, why these data are not regarded.	As we acknowledge in point 1, the foreland unconformity represents a hiatus, primarily due to the passage of the forebulge across the foreland. Accordingly, the forebulge must have passed the study area before any deposition took place, meaning that it was already north of the Geretsried area by the Priabonian. Since the seismic data provide clear evidence that the lower fault array formed later - in the Rupelian, these faults must have originated already within the foredeep. We will adjust our interpretation in the revised manuscript in accordance with these considerations. Please, refer also to our response in the points 20-23.	Changes made in lines 389-426
	3	**page 14 lines 417-426:** In their discussion of the Tilted Molasse, the authors suggest that thrusting in the study area is a direct consequence of flexure-related normal faults, and this thrusting controls tilting. However, on the larger scale of the Bavarian Foreland Basin, the width of the Tilted Molasse is controlled by the presence and depth of a triangle zone. The triangle zone is a rather continuous feature along the Alpine front, while the inherited normal faults are not. The triangle zone seems to be tied to the presence of coarse-grained deposits (see Ortner et al. 2015). Maybe this should be discussed here. Moreover, in the cross sections of Figs. 10 and 11, a Tilted Molasse seems to be absent. From a structural point of view, there is no triangle zone, that could have caused the very mild tilting seen in the seismic sections, and drag across the frontal thrust is not visible. Could it be that the apparent tilting is related to a velocity pull-up, caused by increasing horizontal compaction toward the Alpine front?	We agree with the referee that on the larger scale of the Bavarian Foreland Basin the width of the Tilted Molasse is controlled by the presence of a triangle zone, which is possibly related to the lithological composition of the Late Oligocene to Middle Miocene sediments as presented by Ortner et al. (2015). We also agree with the referee that there is no large triangle zone in the cross-sections of Figs. 10 and 11. Our interpretation of these cross-sections confirms the existing interpretations by Schwerd and Thomas (2003), Thomas et al. (2006), and Ortner et al. (2015) for the eastern part of the Folded Molasse, according to which the deformation at the tip of the Alpine orogen is characterised by a simple overthrust without development of large triangle zones. However, although we do not observe a large triangle zone below the Kirchbichl Thrust in Fig. 11, there is a clear tilting of the upper Cenozoic sequence. We believe it formed due to distributed sub-seismic strain. Such "diffuse" deformation could possibly account for the area increase associated with tilting of higher levels while the lower beds maintain their dip towards the Alps. The average seismic velocities are indeed reported to increase towards the Alps, presumably due to an increase of lateral stress or lithological changes (Greiner and Lohr, 1980). Nevertheless, we doubt that the tilting in Fig. 11 represents a velocity pull-up. If that were the case, we would then have observed a similar velocity pull-up in Fig 10, which depicts a seismic profile (on the right hand side) that was processed using the same workflow as the profile in Fig. 11. We assume that the diffuse deformation below the Kirchbichl thrust that possibly resulted in the tilting, as seen in the cross-section in Fig. 11, accommodated strain as the Alps advanced. In the Geretsried area, such strain was most probably accommodated by thrusting along the Geretrsied thrust fault. Hence, no diffuse sub-seismic deformation and consequent tilting occurred. According to the comments of the referee, in the revised manuscript we will emphasize that the tilting is controlled by a triangle zone on the regional scale, whereas frontal blind thrusting controls deformation on a more local scale. *Reference: Greiner, G., Lohr, J., 1980. Tectonic stresses in the Northern Foreland of the alpine system measurements and interpretation. In: Scheidegger, A.E. (Ed.), Tectonic Stresses in the Alpine-Mediterranean Region. Rock Mechanics/Felsmechanik/Mécanique des Roches. Springer, Vienna, Austria.	Changes made in lines 508-528

Specific comments	4	The recognition of the Geretsried thrust is new. However, Müller (1975/1976) interpreted the structural geometry between the Darching and Miesbach wells with a structural geometry very similar to the present paper. This should be mentioned somewhere. It might have impact on the general interpretation, as it shows that the frontal structure is comparable over a rather broad area.	We thank the referee for providing us information on the structure interpreted by Müller (1975/1976) between the Darching 1 and Miesbach 1 wells, ca. 25 km to the east of the Geretsried survey. This structure was previously unknown to us. It is indeed very similar to the Geretsried Thrust: it truncates the Mesozoic and dies out in the Chattian, splits into two branches and has a comparable vertical offset of ca. 250 m. However, it is unlikely that it represents the eastern continuation of the Geretsried Thrust, which, as has been shown in our paper, dies out rapidly to the east. We believe that this is an separate structure. It could have formed in the similar conditions to the Geretsried area, namely in the presence of flexure-induced faults. Müller (1975/1976) interprets a normal fault truncated by the thrust as antithetic (i.e. dipping forelandward). However, the interpretation of the seismic data in the Dietramszell-Bad Tölz prospect area (1960/1961) shows that faults in the proximity to the Miesbach well 1 are in fact dip hinterlandward (see attached depth map of the Tertiary basis). Futhermore, the N-S oriented profile 6 (see attachment) that runs close to the Miesbach 1 well, shows two antithetic normal faults (α21 and α14) that are vertically decoupled from one another. The upper α21 fault is overprinted by a frontal thrust. High-resolution seismic data, preferably 3D seismic data, would be required to investigate this structure in detail and conclude to which extent it is comparable to the Geretsried Thrust. As suggested by the referee, we will mention the frontal structure interpreted by Müller (1975/1976) in the discussion as follows: "In the GMB, ca. 25 km east of our study area, Müller (1975/1976) interprets a frontal thrust structure with a similar geometry to the Geretsried Thrust that also truncates an early-orogenic normal fault. The fact that the Geretsried Thrust dies out rapidly to the east suggests that the thrust interpreted by Müller (1975/1976) must have formed individually from the Geretsried Thrust."	Included text in lines 492-495
Technical comments	5	**page 1 line 3:** “two normal fault arrays” instead of “two fault arrays”.	The upper fault array, as recognised in the seismic, consists of both normal and reverse faults. We therefore will modify the sentence as follows: "We recognise two fault arrays that are vertically separated by a clay-rich layer — lower normal faults and upper normal and reverse faults."	Changes made in lines 3-4
	6	**page 1 line 3:** “a clay-rich detachment horizon” – The detachment follows a stratigraphic layer, so it is rather a decollement.	According to the Oxford Dictionary of Geology and Earth Sciences (2013), a detachment horizon is "a surface along which overlying rocks have moved in the course of deformation". We therefore agree with the referee that this term in the current context is misleading as we refer to a layer that decouples/separates two fault arrays and not to a surface. In the revised manuscript, we will simply refer to it as "a clay-rich layer".	Changes made in lines 3, 14-15, 590-591
	7	**page 1 line 3:** “A large-scale thrust” - This thrust has not a lot of offset - I would not call it "large-scale".	We will refrain from calling the Geretsried Thrust "large-scale".	Changes made in lines 3, 15
	8	**page 1 line 5:** “(1) initiation of the lower fault array” – better “(1) initiation of the lower normal fault array”.	We will correct the text as follows: “(1) initiation of the lower normal faults”	Changes made in line 6
	9	**page 1 line 6:** “(2) development of the upper fault array” – better “(2) development of the upper normal fault array”.	We will correct the text as follows: “(1) development of the upper normal faults”	Changes made in line 7
	10	**page 1 line 8**: “during the migration of the forebulge (phase 1), foredeep (phase 2)” – these phases have not been explicitely defined in the text; this should be done if this phrase is retained. But see also comments on these specific "phases".	The sentence will not be retained as it is. While it holds true that the distinct faulting phases observed in the Geretsried area are governed by the change in the stress regime as the orogen propagated forwards, we recognize, however, that these phases took place entirely within the foredeep. We will modify this sentence as follows: "These distinct phases document the evolution of the stress field as the Alpine orogen propagated forward across the foreland."	Changes made in lines 8-10

Technical comments	11	**page 2 lines 49-50:** “After a profound hiatus in sedimentation caused by the Late Cretaceous-Palaeocene contractional event as consequence of the change in the African plate motion” - This hiatus is the foreland unconformity (see e.g., Allen et al. 1991), or coincides with it. This should be mentioned (as in Figure 3). In most interpretations, the foreland unconformity marks the passage of forebulge rolling through the flexed European plate. To my knowledge there is no evidence of basement-involved thrusting in the Alpine foreland so close to the Alps in the sense of Kley and Voigt (2015).	As we admit in point 1, the hiatus represented by the foreland unconformity is indeed related to the foreland forebulge. More specifically, the foreland unconformity must represent a composite hiatus due to the local basin inversion during the Late Cretaceous contractional event (Bachmann et al., 1987) and erosion within the transient forebulge from the Pliocene to Middle Eocene (Allen et al., 1997). The contractional deformation in the Late Cretaceous, to which Kley and Voigt (2015) refer, has been recorded by the upthusting of the Bohemian Massif and the Landshut-Neuötting High along the NW—SE wrench faults that delimit the Bohemian Massif and the Landshut-Neuötting High (Bachmann et al., 1987).	Changes made in lines 63-75
	12	**page 3 line 59:** “transgressive sandstones” - It remains unclear, what "transgressive" in this context means. You want to say, that sandstones, carbonates, shales and marls define a transgressive sequence? Or that "transgressive sandstones" overlie the foreland unconfromity? Clarify!	We use the term "transgressive" to imply the sediments that were deposited in the course of marine transgression. We will rewrite the corresponding passage as follows to clarify this: "The foreland basin fill can be divided into Late Eocene ‘Pre-Molasse’ and Oligocene to Miocene ‘Molasse’ sequences (Sissingh, 1997). The deposition of the Pre-Molasse sequence occurred during an early marine transgression and is characterised by non-molasse sedimentation of shallow-marine Basal sandstone and Lithothamnion limestone (Sissingh, 1997; Zweigel, 1998). The overlying Molasse sequence accumulated in the course of two subsequent transgressive-regressive mega-cycles. Traditionally, the Molasse sequence is subdivided into, from older to younger; the Lower Marine Molasse (Untere Meeresmolasse, UMM), the Lower Freshwater Molasse (Untere Süßwassermolasse, USM), the Upper Marine Molasse (Obere Meeresmolasse, OMM), and the Upper Freshwater Molasse (Obere Süßwassermolasse, OSM) (Figs. 1c and 2; von Guembel, 1861). The deposition of the UMM started in the Early Oligocene (Rupelian), during a late marine transgression, as the basin deepened rapidly (Bachmann and Müller, 1982; Sissingh, 1997). It is characterised by the widespread accumulation of pelitic sediments — Fisch shale, Light marly limestone, banded marl, and Rupelian clayey marl (Kuhlemann and Kempf, 2002). Subsequent marine regression in the Mid-Oligocene (Rupelian/Chattian) resulted in deposition of littoral Baustein beds (Diem, 1986; Kuhlemann and Kempf, 2002)."	Changes made in lines 76-94
	13	**page 3 line 60:** “shallow-marine to coastal” - probably better "littoral"	We will change the text accordingly. Please see point 12.	Changes made in lines 92-93

Technical comments	14	**page 3 lines 65-67:** “This suggests that the foreland plate was not affected by further flexure and that the marine transgression during the deposition of OMM was the result of lower sediment input into the basin (Zweigel, 1998; Kuhlemann and Kempf, 2002; Ortner et al., 2015).” - Foreland flexure ended in the eastern part of the basin; the western half continued to subside. Your study area is transitional, but the base of the OMM is still slightly flexed in the TRANSALP section across the foreland (see, e.g., the cross sections of Abele et al. 1955).	After having examined the cross sections of Abele et al. (1955), we admit that the foreland flexure must have continued throughout OMM deposition in the transitional area between the western and eastern German Molasse Basin, as the base of the OMM indeed dips shalowly towards the south in the cross sections 26 and 27 of Abele et al. (1955). We will modify the corresponding passage as follows: "The second transgressive-regressive megacycle began in the Early Miocene (Burdigalian) with transgression of OMM marls over the Aquitanian-Burdigalian unconformity (Fig. 2; Lemcke, 1988; Zweigel et al., 1998). Although the foreland flexuring was ongoing in the GMB during deposition of the OMM (Ortner et al., 2015), the foreland subsidence decreased significantly with the onset of OMM deposition (Zweigel et al., 1998). Despite decreasing subsidence, marine conditions were established in the basin due to a decrease in sediment supply accompanied by the relief reduction in the Eastern Alps (Zweigel et al., 1998; Kuhlemann and Kempf, 2002). By the beginning of the mid-Miocene (Langhian), when deposition of the OSM had started, continental conditions prevailed across the entire GMB (Lemcke, 1988)."	Changes made in lines 103-111
	15	**page 3 line 70:** “Alpine front” - The Alpine front is a line, that cannot incorporate volume. "Alpine wedge" would be more correct.	We will change the text accordingly.	Changes made in lines 113-114
	16	**page 3 line 234:** ”Its stratigraphically higher upper branch” - How can a thrust branch be "stratigraphically higher"? This would only be possible at a specific location, where you have an upper and lower thrust, whatever stratigraphy is.	We will rewrite this as follows: "Its upper branch dips…"	Changes made in line 283
	17	**page 8 line 240**: “At the foot of” – Below?	We agree that this wording might be unclear. We will correct accordingly.	Changes made in lines 304-308
	18	**page 11 line 321:** “This implies a forward-propagating Alpine thrust system, which is most likely.” - Yes, but Ortner et al. 2015 showed that the thrusts of the Subalpine Molasse are hinterland breaking, where a clear sequence can be recognized. Maybe the Geretsried thrust marks the turnaround from foreland- to hinterland-breaking.	We acknowledge the interpretation of Ortner et al. 2015 in that the thrusts of the Subalpine Molasse are hinterland-breaking. The fact that the Geretsried Thrust is the foremost thrust of the Alpine thrust system indeed does not imply that it is the youngest thrust. We agree that it could mark the turnaround from foreland- to hinterland-breaking. Unfortunately, we lack seismic observation of the growth strata above the thrust-related Geretsried Fold to put a temporal constrain on the thrust activity and thus confirm this proposition. In the revised manuscript, we will remove the following sentence: “This implies a forward-propagating Alpine thrust system, which is most likely.” Also, in the preceding sentence - "However, we hypothesise that the Geretsried thrust was contemporaneous with or succeeded the frontal thrusts of the Folded Molasse, because it is rooted below the Folded Molasse and is thus kinematically related to the frontal thrusts." we will reduce our interpretation of timing to "contemporaneous".	Changes made in line 381, 384
	19	**page 11 line 336:** “lower fault activity” – better “activity of the lower fault array”	The sentence that contains this phrase will be removed from the manuscript as the corresponding paragraph will be rewritten to comply with the comment of the referee in the point 20.	The corresponding sentence is removed

Technical comments	20	**page 11 line 337:** "initiated as the forebulge, the region of maximum flexure, reached the Geretsried area in the early Rupelian" - This is difficult. When the forebulge is related to the foreland unconformity (depicted in Fig. 3) and the normal faults are related to the forebulge, then normal faulting should have initiated during continental conditions and erosion. However, fault activity might have extended into the Rupelian, when the Alpine wedge still moved onto the European plate rapidly (see e.g., Pfiffner, 1986), and flexure was ongoing.	Considering our response to the comments of the referee in points 1 and 2, we conclude that the normal faulting of both fault arrays must have occurred entirely within the foredeep during the foreland flexuring. Below is our revised interpretation of the faulting phases in the Rupelian and the Chattian. "The longitudinal strike of the lower and upper faults, with respect to the Alpine orogenic front, implies that they formed due to the flexure-induced deformation on the foredeep slope. It has been recognized that during foreland flexuring, the upper part of the bending plate experiences extension, the lower part — compression, and a central horizon is neutral (Turcotte and Schubert, 1982; Price and Cosgrove, 1990). Within the region of maximum flexure (i.e., foreland forebulge), elastic bending facilitates an extensional stress field with an effective minimum stress oriented perpendicular to the trend of the foredeep (Bradley and Kidd, 1991; Bachmann and Müller, 1992; Londoño and Lorenzo, 2004; Langhi et al., 2011). As the syn-orogenic load within the foredeep increases towards the orogen, the sub-vertical maximum principle stress increases as well. Consequently, normal faults form in a basinward position with respect to the region of maximum flexure, striking parallel to the foredeep axis (Tavani et al., 2015). The first faulting phase initiated in the Early Oligocene (early Rupelian) as evidenced from the seismic data. At this time, the GMB was characterised by a limited sediment supply (Zweigel et al., 1998). Hence, we imply that the magnitude of the sub-vertical stress was low as the lower fault array formed. Presumably, the lower normal faults occurred in the distal foredeep, close to the region of maximum flexure, where the magnitude of the horizontal compression was still small enough for the differential stress to cause normal faulting. As the Alpine orogen moved forward, the magnitude of the horizontal stress component increased, resulting in termination of normal faulting in the late Rupelian. The second faulting phase occurred in the Late Oligocene (Chattian). Zweigel et al. (1998) document a drastic increase of sedimentation rates at this time due to the increase of the topographic relief in the Alpine orogen. A rapid thickening of the sedimentary load must have resulted in an increase of the vertical stress that eventually exceeded horizontal compression, resulting in renewed normal faulting. The existence of a sub-vertical maximum stress in the Late Oligocene—Early Miocene is also implied from the build-up of overpressure in the Rupelian sequence that is related to high sedimentation rates during this time (Müller et al., 1988; Müller and Nieberding, 1996)."	Changes made in lines 393-427
	21	**page 11 line 343:** "By the Chattian times, the foreland foredeep approached the study area," - I do not understand. The complete foreland sequence is in the foreland foredeep. The thickness of all units below the OMM diminishes toward the forebulge to the N (see lines 62-68, and references cited there; see also cross sections of Abele et al. 1955).		
	22	**page 11 line 344:** "This" - To which part of the preceding sentence does "this" relate? Neither possibility makes any sense - rapid sedimentation cannot be caused by the approach of the foredeep (see remark there), and not caused by the thickness increase (being an effect and not a cause). Reformulate and clarify. Probably the arguments in this whole paragraph need to be reconsidered, reformulated and reordered.		
	23	**page 12 lines 346-347:** "Increasing sedimentary load towards the orogen produced an increase in the vertical stress magnitude (Drews et al., 2018) and therefore favoured normal faulting." - See last remark. This information needs to be given before you argue that pressure distribution may support your idea.		

Technical comments	24	**page 14 Lines 422-423:** "We postulate that the varying amplitude of the tilted zone from west to east must be controlled by the occurrence of early-orogenic normal faults that facilitate thrusting. In the Geretsried area and south of it, the Geretsried Thrust accommodated shortening and thereby prevented large-scale folding in front of the propagating Alpine thrust sheets." - (1) In the absence of available seismic data in the area, I put the northern limit of the Tilted Molasse at the northern limit of tilting as shown in the cross sections of Abele et al. (1955). (2) On the scale of the Bavarian Molasse, the width of the Tilted Molasse is mostly controlled by the presence and depth of a triangle zone. The triangle zone is a rather continuous feature along the Alpine front, while the inherited normal faults are not. The triangle zone seems to be tied to the presence of coarse-grained deposits (see Ortner et al. 2015). Maybe this should be discussed here. (3) In the cross sections of Figs. 10 and 11, a Tilted Molasse seems to be absent. From a structural point of view, there is no triangle zone, that could have caused the very mild tilting seen in the seimic sections, and drag across the frontal thrust is not visible. Could it be that the apparent tilting is related to a velocity pull-up, caused by increasing horizontal compaction toward the Alpine front?	(1) The seismic cross-section in Fig. 10 does not confirm interpretation by Abele et al. (1955), shown in the respective profile 7, with regard to the shape of the Tilted Molasse. (2) We agree that the Tilted Molasse is controlled by the triangle zone on the scale of the Bavarian Molasse. (3) We clearly see tilting in the cross-section of Fig. 11, below the Kirchbichl Thrust. We believe it formed due to the distributed sub-seismic strain that can account for the area increase associated with tilting of higher levels while the lower beds maintain their dip towards the Alps. The average seismic velocities are indeed reported to increase towards the Alps, presumably due to an increase of lateral stress or lithological changes (Greiner and Lohr, 1980*). Nevertheless, we doubt that the tilting in Fig. 11 represents a velocity pull-up. If this were the case, we would then have observed a similar velocity pull-up in Fig 10, which depicts a seismic profile (on the right hand side) that was processed using the same workflow as the profile in Fig. 11. *Reference: Greiner, G., Lohr, J., 1980. Tectonic stresses in the Northern Foreland of the alpine system measurements and interpretation. In: Scheidegger, A.E. (Ed.), Tectonic Stresses in the Alpine-Mediterranean Region. Rock Mechanics/Felsmechanik/Mécanique des Roches. Springer, Vienna, Austria.	Changes made in lines 508-528
	25	**page 14 lines 423-425:** "In the Geretsried area and south of it, the Geretsried Thrust accommodated shortening and thereby prevented large-scale folding in front of the propagating Alpine thrust sheets." - Keep in mind that there is almost no offset across this thrust. If there would be a few kilometers of offset, then there would be folding for sure.	By large-scale folding we mean large-wavelength tilting of the Molasse sediments. There is still a fault-related folding in the hangingwall of the Geretsried Thust.	Changes made in lines 523-526
	26	**page 15 line 444**: "Walsch" – It is "Walsh"	We will correct the misspelling.	Corrected
	27	**page 15 line 453**: "Walsch" - Again, "Walsh"!		
Figures	28	**Figure 2**: Strange that all normal faults die out in the deepest layer. Distinguish wells and faults graphically!	The schematic cross-section in Figure 2 depicts only basement-rooted faults that were interpreted in the TRANSALP seismic profile. We now distinguish the wells from the faults graphically using different symbols.	Figure 2 (Figure 1c in the revised manuscript) is modified

Figures	**29**	**Figure 3:** In the column “Local stratigraphy”: **a.** “Laminated marl” instead of “Laminated barl” **b.** Chattian sandstone: A significant part of these Chattian sands, and the "Aquitanian beds" are in fact an alternation of sands, carbonates, coal and shales, and has been termed the Cyrena beds, a brackish facies transitional between the continental USM and the marine UMM. This should probably be mentioned somewhere. **c.** Rupelian clay Banded marl Heller Mergelkalk Fish shale mixture of German and English here. The German terms are "Heller Mergelkalk", "Bändermergel" and "Tonmergel". Either translate all of them, or use the German terms consistently. **d.** Tonmergel would be Rupelian clayey marl in English, 'Rupelian clay' is misleading.	**a.** We will correct the typo in "Laminated marl". **b.** In the revised figure, we will refer to the "Chattian beds" as part of the Lower Brackish Molasse (UBM) instead of the "Chattian sandstone" as part of the USM. In the revised text, in chapter "Geological Setting", we will add the following sentences to explain what is meant by "Chattian and Aquitanian beds": "In the Late Oligocene to Early Miocene (Chattian and Aquitanian), continental conditions were established in the western basin part, and thus the deposition of the USM, while to the east of Munich marine sedimentation continued in the deeper part of the basin. The central GMB was dominated by coastal to shallow-marine settings, resulting in accumulation of the transitional Lower Brackish Molasse (Untere Brackischmolasse, UBM). It is composed of the Chattian and Aquitanian beds, termed the Cyrena beds, — an alternation of calcareous sandstones, marlstones, limestones, and coal (Freundenberger and Schwerd, 1996)." **c.** We will use the English translations of the lithological units only. The German term "Heller Mergelkalk" will be changed to "Light marly limestone". **d.** We will use the term "Rupelian clayey marl" instead of the term "Rupelian clay" everywhere in the revised text.	Figure 3 (Figure 2 in the revised manuscript) is modified; Text included in lines 94-99; Terms "Heller Mergelkalk" and "Rupelian clay" are changed accrodingly
	30	**Figure 18:** You might want to color negative and positive throw differently	We will change the colour of the negative throw to distinguish it from the positive throw.	Figure 18 (Figure 9 in the revised manuscript) is modified
	31	**Figure 20:** lower row of sketches: How can the basement fold be with such a short wavelength? I really have problems imagining this. In such a scenario, folding of the basement would be one of the controlling factors. This should be mentioned and discussed in the text. In the seismic lines there seems to be less folding.	The folding in the basement cannot indeed be of such a short wavelength. In this respect, the lower sketches misrepresent the reflection configuration shown in the seismic close-ups. We will modify the sketches accordingly.	Figure 20 (Figure 10 in the revised manuscript) is modified

Editorial Comments: Virginia Toy (University of Mainz)			
Point No.	**Comment of the referee** (line numbers refer to the initial version of the manuscript)	**Response of the authors**	**Implemented changes** (line numbers refer to the annotated version of the revised manuscript)
1	In any revision you make after we get more reviewers to comment, please try to make this less 'local'. By that, I mean that some of the location names that you are currently using, and also the geological time scale, are specifically European. There are two mountain chains called the Alps on the planet and you need to specify this was the 'European Alpine deformation front'. Furthermore, when are the Rupetian and Chattian? You could introduce a citation to the time scale that you are using, but it would be much simpler just to give them time frames in millions of years.	We will specify in the "Introduction" chapter that in this paper we are referring to the European Alpine deformation front. When referring to the geological time, we will use the epoch time unit followed by the age time unit in brackets; e.g.: Early Oligocene (Rupelian).	Changes made in lines 41, 604
2	Tenses. Please carefully examine whether you were talking about the present or the past tense. I generally try to write in the present tense rather than the past – you have mostly done the latter, but in a rather inconsistent way.	We will revise the manuscript for a consistent use of tenses.	Changes made with respect to the choice of tenses.

Additional author changes

Some further minor changes by the authors, which were not requested by the referees, comprise only improvements of wording and are marked in the annotated version of the revised manuscript.

Multiphase, decoupled faulting in the southern German Molasse Basin — evidence from 3D seismic data

Vladimir Shipilin[1,2], David C. Tanner[1], Hartwig von Hartmann[1], and Inga Moeck[1,2]

[1]Leibniz Institute for Applied Geophysics, Stilleweg 2, D-30655 Hannover
[2]Georg August University Göttingen, Goldschmidtstr. 3, D-37077 Göttingen

Correspondence: Vladimir Shipilin (Vladimir.Shipilin@leibniz-liag.de)

Abstract. We use three-dimensional seismic reflection data from the southern German Molasse Basin to investigate the structural style and evolution of a geometrically decoupled fault network in close proximity to the Alpine deformation front. We recognise two fault arrays that are vertically separated by a clay-rich ~~detachment horizon. A large-scale thrust~~ layer — lower normal faults and upper normal and reverse faults. A frontal thrust fault partially overprints the upper fault array. Analysis of seismic stratigraphy, syn-kinematic strata, throw distribution, and spatial relationships between faults suggest a multiphase fault evolution: (1) initiation of the lower ~~fault array~~ normal faults in the Upper Jurassic carbonate platform during the ~~Rupelian~~Early Oligocene, (2) development of the upper ~~fault array~~ normal faults in the Cenozoic sediments during the ~~Chattian~~Late Oligocene, and (3) reverse reactivation of the upper normal faults and thrusting during the mid-Miocene. These distinct phases document the evolution of the stress field ~~during the migration of the forebulge (phase 1), foredeep (phase 2) and the toe of the orogenic front (phase 3) across the investigated area~~as the Alpine orogen propagated across the foreland. We postulate that ~~phase 2 was controlled by the vertical stress gradients, whereby a lower horizontal stress component within the Cenozoic sediments~~ interplay between the horizontal compression and vertical stresses due to the syn-sedimentary loading resulted in the intermittent normal faulting. The vertical stress gradients within the flexed foredeep defined the independent development of the upper faults above the lower faults~~. Mechanical~~, whereas mechanical behaviour of the clay-rich ~~horizon~~ layer precluded the subsequent linkage of the fault arrays. ~~A large-scale thrust~~ The thrust fault must have been facilitated by the reverse reactivation of the upper normal faults, as its maximum displacement and extent correlate with the occurrence of these faults. We conclude that the evolving tectonic stresses were the primary mechanism of fault activation, whereas the mechanical stratigraphy and pre-existing structures locally governed the structural style.

1 Introduction

In the last decade, there has been an increasing interest in foreland basins because of the existence of deep aquifers that might host geothermal resources (e.g., Schulz et al., 2004; Weides and Majorowicz, 2014). Understanding of tectonic evolution and fault kinematics is crucial to evaluate potential geothermal reservoirs, which at depths below 3 km are primarily controlled by fault and density of interconnected fractures (Moeck, 2014).

Foreland basins have complex deformation structures that range from normal faults towards the foreland to contractional and inverted faults near the orogenic front (DeCelles and Giles, 1996; Tavani et al., 2015). Such a deformation pattern shows that the basin is subject to a variety of stress states that develop during the lithospheric flexuring, subsidence, and sedimentation as the orogenic front progresses forward. Locally, the stress states may be modified by inherited structures, such as pre-existing faults (Tavani et al., 2015; Wibberley et al., 2008), and differences in mechanical behaviour of rock layers (Ferrill et al., 2017). The resultant composite structural history can ~~only~~ be correctly deciphered using a three-dimensional approach, such as can be derived from three-dimensional seismic datasets.

~~Our working area is within~~ The focus of this work is an in-depth analysis of deformation structures in the southernmost part of a typical foreland basin system, the German Molasse Basin~~, near the town of Geretsried, 30 km south of Munich (Fig. 1).~~ . A number of basin-scale structural studies were carried out in the '80s and '90s, based on a large amount of 2D seismic data acquired for hydrocarbon exploration over decades (e.g., Bachmann et al., 1982, 1987; Müller et al., 1988; Bachmann and Müller, 1992). The increasing interest in geothermal exploitation in recent years and therefore the acquisition of 3D seismic data, have allowed more detailed studies of the complexly deformed areas (e.g., Lüschen et al., 2011; von Hartmann et al., 2016; Budach et al., 2017). Nevertheless, the tectonic and stratigraphic factors controlling the evolution of the structure of the German Molasse Basin have not been fully described as yet.

~~The focus of this work is an in-depth analysis of deformation structures in the Geretsried study area . Our~~ Using a 3D seismic reflection dataset, acquired in the area of Geretsried, 30 km south of Munich (Fig. 1), our aim is to understand the complex structure and tectonic evolution of an area proximal to the European Alpine deformation front. To achieve this, we ~~use 3D seismic reflection~~ analyse the seismic data to (i) reconstruct the temporal and spatial evolution of the fault network within the ~~Molasse~~ foreland basin sequence and its Mesozoic substratum, and (ii) evaluate the impact of the evolving stress field, pre-existing deformation structures, and mechanical stratigraphy on fault evolution, structural style, and kinematic interactions between faults.

2 Geological Setting

The German Molasse Basin (GMB) is part of the North Alpine Foreland Basin (~~Figs~~Fig. 1~~and 2~~) that evolved on the subducting European margin ~~, in front of the Alps, since the Late Eocene (Lemcke, 1973; Bachmann et al., 1982). The Cenozoic deposits~~ in response to the Late Eocene Alpine collision (Frisch, 1979; Lemcke, 1973; Bachmann et al., 1982; Ziegler et al., 1995). Orogenic loading and consequent flexure of the foreland ~~basin unconformably overlie the peneplained Mesozoic sedimentary basement (Fig. 3) and locally, Permo-Carboniferous clastic sediments and crystalline rocks (Lemcke, 1973; Sissingh, 1997)~~ plate created a wedge-shaped basin fill in front of the advancing Alps (Allen et al., 1991; Bachmann and Müller, 1992). Flexural subsidence was accompanied by the formation of longitudinal (i.e., foredeep-parallel) normal faults (Lemcke, 1988; Bachmann et al., 1982; .

From ~~Jurassic to mid-Cretaceous~~the Jurassic to mid-Cretaceous, the region of the future ~~Molasse Basin~~ GMB evolved as a ~~proximal~~ passive margin (Frisch, 1979; Ziegler, 1990; Pfiffner, 1992). Submergence of the southern European ~~shelf~~

by the Tethys Ocean margin in the Jurassic led to the deposition of Lower and Middle Jurassic marine shales and the establishment of an Upper Jurassic carbonate platform (Meyer & Schmidt-Kaler, 1990). In the southeast, the carbonate platform is overlain by partially preserved, Cretaceous , Upper Jurassic carbonates on a gently sloping, shallow platform (Meyer and Schmidt-Kaler, 1990). Subsequent phases of eustatically-induced regression and transgression in the Cretaceous resulted in sedimentation of shallow-water carbonates, glauconitic sandstone, and deep-water marls and shales (Fig. 3; Bachmann et al., 198 (Fig. 2; Bachmann et al., 1987).

After a profound hiatus in sedimentation The sedimentation of the Mesozoic passive margin terminated with the onset of Late Cretaceous compressional deformation. It is widely accepted to have been caused by the Late Cretaceous-Palaeocene contractional event as consequence of the change in the African plate motion (Kley and Voigt, 2015), deposition resumed in the Late Eocene (Ziegler et al., 1995; Sissingh, 1997). It marks the inception of the foreland basin inception of the NW-directed Alpine thrusting (Ziegler, 1987, 1990). However, Kley and Voigt (2015) argue that the Late Cretaceous pulse of the NNE–SSW-oriented contraction reflects the change of Africa's motion relative to Europe from south-easterly to north-easterly. As the result of the Late Cretaceous intraplate contraction, the Mesozoic passive margin was subjected to inversion and erosion (Bachmann and Müller, 1991; R . Erosion continued throughout the Palaeocene to Middle Eocene (Lemcke, 1981) due to the subsequent uplift of the flexural forebulge that migrated across the foreland in advance of the Alpine orogen (Allen et al., 1991). The Late Eocene flexural subsidence in the GMB marked the onset of foredeep sedimentation. As the Alpine orogen continued to move forward, the basin fill progressively onlapped in NW-direction onto the truncated Mesozoic basement and locally, Palaeozoic rocks (Lemcke, 1988; Freudenberger and Schwerd, 1996), forming an angular basal unconformity, referred to as the forebulge unconformity by Allen et al. (1991).

The foreland basin fill can be subdivided into Late Eocene 'Pre-Molasse' and Oligocene to Miocene 'Molasse' sequences (Sissingh, 1997). The deposition of the Pre-Molasse sequence occurred during an early marine transgression and is characterised by non-molasse sedimentation of shallow-marine Basal sandstone and Lithothamnion limestone (Sissingh, 1997; Zweigel et al., 1998) . The overlying Molasse sequence accumulated in response to the Euro-Adriatic collision (Frisch, 1979; Allen et al., 1991; Ziegler et al., 19 . Loading and consequent flexure of the European foreland plate created a wedge-shaped basin fill (Allen et al., 1991). Flexural subsidence was accompanied by the formation of longitudinal (i. e., foredeep-parallel) normal faults (Lemcke, 1988; Bachmann et al., 1982 .

The Cenozoic Molasse cover was deposited in the course of two major subsequent transgressive-regressive cycles and can be megacycles. Traditionally, the Molasse sequence is subdivided into, from older to younger; the Lower Marine Molasse (Untere Meeresmolasse, UMM), the Lower Freshwater Molasse (Untere Süßwassermolasse, USM), the Upper Marine Molasse (Obere Meeresmolasse, OMM), and the Upper Freshwater Molasse (Obere Süßwassermolasse, OSM) (Figs. 2 & 3; von Guembel, 1861) . The UMM is Late Eocene to Early Oligocene in age and consists of transgressive sandstones, shelf carbonates, and deep-water shales and marls (Lemcke, 1988; Sissingh, 1997). The (Figs. 1c and 2; von Guembel, 1861).

The deposition of the UMM started in the Early Oligocene (Rupelian) during a late marine transgression, as the basin deepened rapidly (Bachmann and Müller, 1992; Sissingh, 1997). It is characterised by the widespread accumulation of pelitic sediments — Fisch shale, Light marly limestone, Banded marl, and Rupelian clayey marl (Kuhlemann and Kempf, 2002).

Subsequent marine regression in the Mid-Oligocene ~~accumulation of regressive, shallow-marine to coastal Baustein sandstones marks the transition from UMM to USM (Diem, 1986). These are overlain by fluvial~~ (Rupelian/Chattian) resulted in deposition of littoral Baustein beds (Diem, 1986; Kuhlemann and Kempf, 2002). In the Late Oligocene to Early Miocene (Chattian and Aquitanian~~sandstones.~~), during the deposition of the USM, continental conditions were established in the western basin part, while marine sedimentation continued in the deeper part of the basin, to the east of Munich. The central GMB was dominated by coastal to shallow-marine setting, resulting in accumulation of the transitional Lower Brackish Molasse (Untere Brackwassermolasse, UBM). It is composed of the Chattian and Aquitanian beds, termed the Cyrena beds, — an alternation of calcareous sandstones, marlstones, limestones, and coal (Freudenberger and Schwerd, 1996).

~~In Early to Middle Miocene times, thrusting of the Alps abated and subsidence rates decreased (Zweigel et al., 1998). Despite decreasing subsidence, the~~ The second transgressive-regressive ~~cycle~~ megacycle began in the ~~Burdigalian~~ Early Miocene (Burdigalian) with transgression of OMM marls over the Aquitanian-Burdigalian unconformity ~~(Fig. 3; Lemcke, 1988; Zweigel et al., 1998~~ . ~~At the same time, the basin-infill geometry changed from wedge-shaped to tabular (Fig. 2; Kuhlemann and Kempf, 2002). This suggests that the foreland plate was not affected by further flexure and that the marine transgression during the deposition of OMM was the result of lower sediment input into the basin (Zweigel et al., 1998; Kuhlemann and Kempf, 2002; Ortner et al., 2015)~~ (Fig. 2; Lemcke, 1988; Zweigel et al., 1998). Although the foreland flexuring was ongoing in the GMB during deposition of the OMM (Ortner et al., 2015), the foreland subsidence decreased significantly with the onset of OMM deposition (Zweigel et al., 1998) . Despite decreasing subsidence, marine conditions were established in the basin due to a decrease in sediment supply accompanied by the relief reduction in the Eastern Alps (Zweigel et al., 1998; Kuhlemann and Kempf, 2002). By the beginning of the ~~Langhian, terrestrial~~ mid-Miocene (Langhian), when deposition of the OSM had started, continental conditions prevailed across the entire GMB ~~, as the OSM was deposited~~ (Lemcke, 1988).

At the southern basin margin, the Folded (Subalpine) Molasse was formed by thrusting and incorporation of the proximal foreland basin sediments into the Alpine ~~front (Fig. 2; Bachmann et al., 1987; Reinecker et al., 2010; Ortner et al., 2015)~~ wedge (Fig. 1c; Bachmann et al., 1987; Reinecker et al., 2010; Ortner et al., 2015). Thermochronological data suggest that the thrusting in the Folded Molasse continued into the Late Miocene (von Hagke et al., 2015). From c. 8.5 Ma onwards, the GMB experienced isostatically-induced uplift and erosion (Lemcke, 1973).

3 Database

The main database for this investigation is a Kirchhoff pre-stack, depth-migrated, 3D seismic reflection survey. It was acquired in 2010 for geothermal exploration and covers an area of c. 40 km^2 in the southern part of the GMB (Fig. 1). The seismic volume has a record length of 5000 ms two-way travel time (TWT) with a 36-fold bin size of 25 m by 25 m. It is displayed with SEG standard polarity; that is, positive and negative impedance contrasts are depicted as peaks (red) and troughs (blue), respectively. The vertical stratigraphic resolution ranges from c. 20 m within the Cenozoic Molasse sediments to c. 55 m at the base of the carbonate platform. Additionally, we used paper copies of two c. 7 km long seismic profiles that were acquired in 1987 to investigate the deformation style at the transition between the Foreland Molasse and the Folded Molasse. The

profiles are located south and southeast of the 3D seismic survey area (Fig. 1b) and therefore allowed us also to investigate the southward extent of the structures identified within the 3D seismic survey.

The seismic reflection data are supplemented by a vertical seismic profile and formation top data from the only borehole available within the study area — GEN-1, down to the intermediate level of the Upper Jurassic carbonate platform (Fig. ~~3~~2). We used time-to-depth picks obtained from the vertical seismic profile to calibrate the interval migration velocities. The resultant velocity model was used for time-to-depth conversion.

4 Methodology

4.1 3D seismic interpretation

The 3D seismic reflection survey was interpreted in the time domain using Schlumberger Petrel® seismic interpretation software. We used the vertical seismic profile data to tie well stratigraphy to the seismic dataset. This provided age constraints for seven seismic horizons that were mapped across the dataset from the top of the Purbeckian limestone, which corresponds to the top Berriasian, up to the highest seismically recognizable horizon — top Aquitanian (Fig. ~~3~~2). An additional horizon — the inferred base of the carbonate platform (top Callovian) — was also interpreted. For this interval, there is no well control and vertical seismic resolution is poor. We picked a prominent positive-phase reflection that can be considered the base of the carbonate platform, given the reported 600–650 m thickness of the latter (Lemcke, 1988), and expected strong acoustic impedance contrast due to a change in lithology, and therefore velocity and density, from the Upper Jurassic carbonates to the Middle Jurassic clastics.

To better detect faults, we implemented a fault enhancement filter ~~to~~ on the seismic dataset and used seismic volume attributes, such as variance and curvature. The fault enhancement filter suppresses random noise and enhances amplitudes at fault locations, resulting in sharper fault edges. Hence, high variance anomalies became more pronounced, highlighting faults that have discrete offsets. The curvature attribute was used to infer the presence of faults where a discrete offset is succeeded by a 'curved' reflection shape. Such curved geometries could be the seismic expression of subseismic conjugate faulting, plastic deformation in the presence of mechanical stratigraphy, or an imaging artefact due to lateral changes of seismic velocities at faults (Marfurt, 2018).

Subsequently, the variance and curvature volumes were co-rendered to map the full extent of the faults. The faults were traced on time-slices in multiattribute display and then mapped on vertical sections in reflectivity display. The vertical sections were preferentially oriented perpendicular to the strike of the faults, with a line spacing of 75–100 m.

4.2 Structural Modelling

In addition to 3D seismic interpretation of key stratigraphic horizons and faults, we created a consistent 3D structural model to analyse the three-dimensional relationship between faults and sedimentation. For the modelling, the interpreted stratigraphic horizons and faults were depth-converted and imported as ASCII point-sets into SKUA-GOCAD® (Paradigm Ltd., 2017). We

used two interpolation methods to construct triangulated surfaces from point-sets; (i) direct triangulation for fault modelling, and (ii) discrete smooth interpolation for stratigraphic surface modelling. The former method directly tessellates the surfaces, whereby the interpreted points are used as hard constraints to form the vertices of triangles. In the latter method, the interpreted points are not directly part of the surface. Instead, the discrete smooth interpolation creates a trend surface, whereby the interpreted points are honoured as soft constraints in a least-square sense (Mallet, 2002). The resultant surface has a minimum distance to the points and is therefore representative of the original interpretation. We chose the latter method for stratigraphic horizon modelling, because it minimises the artificial roughness of the surfaces, which is inherited from the interpretation due to a large amount of data points. To model displacement of stratigraphic horizons along faults, we used the 'Modelling Horizon-to-Fault Contacts' module in the 'Structural Modelling' workflow. It consists of two steps:

1. Calculation of a horizon-to-fault contact line between the current geometry of the horizon and the fault. New irregularly spaced points are created within the horizon surface, along the contact with the fault.

2. Construction of a faulted horizon. The horizon surface is opened along the fault plane using the discrete smoothing interpolation algorithm. The original point-set is used as control points to allow the interpolation algorithm to keep the faulted horizon as close as possible to the original point-set. Points within the vicinity ~~to~~ of the fault are considered of a high interpretation uncertainty and therefore we excluded the points within 50 m of the fault from the interpolation process.

From the structural model, we used the following tools to obtain temporal and spatial constraints on the evolution of the investigated fault network:

(i) Isochore maps of the key stratigraphic units. This tool allows us to analyse thickness variations across faults to infer their syn-depositional activity (e.g., Jackson and Larsen, 2009; Tvedt et al., 2013; Ziesch et al., 2017). The isochore maps were generated by computing vertical distance between the modelled horizon surfaces bounding a stratigraphic unit and projecting this information (as a scalar value at every triangle node) onto the basal horizon. The algorithm calculates the vertical distance from the basal horizon surface to the nearest top horizon surface, so that overlapping of surfaces due to contractional faulting does not produce an artefact. The major limitation of this method are the computational artifacts associated with the gaps on the top surface produced by normal faults. The computational algorithm attributes zero values to the area of the basal horizon surface directly beneath the fault gap and interpolates minimal values to the adjacent regions to avoid abrupt thickness change to zero meters. This results in significant thinning of a stratigraphic unit towards a fault, which is in fact a computational error.

(ii) ~~Juxtaposition (Allan) diagrams~~Allan maps (juxtaposition diagrams). These diagrams show the throw distribution in a view ~~parallel~~ perpendicular to the fault surface and therefore provide insight into the growth and linkage history of the fault (Allan, 1989). A juxtaposition diagram is constructed by projecting fault cut-offs of the stratigraphic horizons onto a vertical plane that is perpendicular to the pole of the fault surface. To quantify throw distribution, we created polylines at fault cut-offs with nodes at a constant interval of 50 m and plotted them ~~onto~~ on a depth vs. fault strike-length diagram. Additionally,

we produced vertical throw distribution plots (t-z plots) for selected faults to quantify their growth and propagation (e.g., Cartwright et al., 1998; Baudon and Cartwright, 2008a, b, c; Tvedt et al., 2013).

~~(iii) Stereographic projections of the poles of fault surfaces to characterise the geometry of the faults (von Hartmann et al., 2016; Ziesch e~~

5 Results

5.1 Seismic stratigraphy

The good quality of the seismic data, along with the lithological constraints of the mapped horizons enabled us to establish a seismic-stratigraphic framework of the study area, and characterise depositional patterns of the basin fill. The identified horizons define seven seismic-stratigraphic units, as shown on the representative seismic profiles in ~~Figures 4, 5, and 6~~Figure 3. The stratigraphic framework (Fig. 3) qualitatively depicts the mechanical stratigraphy of the identified units, providing information on the competence contrast rather than actual rock strength. The latter is difficult to assess for rocks at the time they were deformed (Ferrill et al., 2017). The stratigraphic units are specified as either competent or incompetent, based on the published interpretation of their mechanical behaviour from outcrop and well data (Fischer, 1960; Müller, 1970; Budach et al., 2017) and on the mechanical properties from literature, e.g., von Hartmann et al. (2016). Figure 3 shows also inferred locations of detachment horizons (Bachmann et al., 1982; Müller et al., 1988; Ortner et al., 2015; von Hartmann et al., 2016).

Unit 1 ~~has a heterogeneous, low-frequency seismic expression that~~ corresponds to the Upper Jurassic carbonate platform that has a heterogeneous, low-frequency seismic expression. Seismic patterns in its lower part are characterised by c. 150 m thick relatively continuous, moderate-amplitude reflections, whereas seismic patterns in the middle and upper parts exhibit alternating chaotic to sub-parallel, low to moderate-amplitude reflectivity. The base of the unit is marked by a low frequency, locally incoherent reflection interpreted as top Callovian. In contrast, the upper-bounding reflection, top Berriasian, is generally continuous and easy to correlate even when extensively faulted.

Units 2 and 3 constitute a package of continuous, low-frequency, and high-amplitude seismic events that reflect contrasting lithologies. Unit 2 corresponds to mechanically incompetent Cretaceous shales and marls and a thin layer of sandstone, whereas Unit 3 represents competent ~~Priabonian sediments (~~Upper Eocene (Priabonian) sediments — Basal sandstone and Lithothamnion limestone ~~)~~ (Budach et al., 2017). Unit 2 thickens substantially southwards (from c. 90 m to c. 170 m), which is in agreement with the regional northward-oriented truncation of the Cretaceous sediments. In contrast, Unit 3 only slightly thickens to the south.

Low amplitude, semi-continuous reflections of Unit 4 onlap onto the upper boundary of Unit 3 — top Priabonian. It is the most prominent reflection across the survey, marking an abrupt change from shallow-marine to deep-marine sedimentation during the ~~Rupelian~~Early Oligocene (Rupelian). It also marks the transition from the competent Unit 3 to an incompetent Unit 4 (Fischer, 1960; Müller, 1970; Budach et al., 2017; von Hartmann et al., 2016). Poor reflectivity of Unit 4 is explained by low impedance contrast within the Rupelian ~~clays and~~ clayey marls. At the top, the unit is marked by toplap terminations below a

continuous, moderate-amplitude negative reflection — top Rupelian (Fig. ~~5~~3e, f). The unit shows a profound thickness increase from c. 600 m in the north to c. 800 m in the south.

Unit 5 is characterised by parallel, highly continuous and high amplitude reflections that correspond to more competent Baustein beds (Budach et al., 2017). Strong impedance contrasts within the unit are attributed to interlayering of sandstones and marls. Unit 5 has a uniform stratigraphic thickness across the survey.

Unit 6 overlies Unit 5 in a concordant manner. While its lowest part has similar reflection characteristics to Unit 5, reflectivity and continuity of seismic events of the middle part decrease upwards. This is due to the increasing marl content, as evidenced by the GEN-1 well (Fig. ~~3~~2). Thus, mechanical competence of the unit also decreases upwards. The uppermost part of the unit is characterised by continuous, high-amplitude reflections, which are caused by sandstone-marl alternations. To the south, ~~bedding changes dip direction~~ the dip direction of bedding changes from southward to northward due to the folding-related deformation. Unit 6 increases in thickness to the south, giving it a wedge-shape geometry.

The seismic response of Unit 7 consists of moderately continuous, low to moderate amplitude reflections. The frequency of the seismic events increases ~~upward~~ upwards within the unit. It corresponds to the Aquitanian sandstone-marlstone series that show no thickness change.

5.2 Structural framework

The 3D structural model shows that the study area contains two distinct fault arrays that are geometrically (vertically) decoupled and a ~~large~~ thrust (Fig. ~~7~~4). We term these decoupled fault arrays the lower and the upper. In the former, faults do not extent upwards beyond clay-rich Unit 4 (Rupelian), and in the latter, faults terminate downwards within Unit 4 (Fig. ~~4~~3b, d). The geometry and distribution of the lower faults is depicted on the multiattribute and depth-structure maps of top Turonian (~~Figs. 8~~Fig. 6a, b), while the geometry and distribution of the upper faults is depicted on the multiattribute and depth-structure maps of top Rupelian (Figs. ~~8~~6c, d) and top Baustein beds (~~Figs. 8~~Fig. 6e, f). The strike direction of the thrust is shown on the multiattribute and depth-structure maps of top Baustein beds (~~Figs. 8~~Fig. 6e, f).

5.2.1 Lower fault array

The lower fault array consists of normal faults that are parallel with respect to the Alpine deformation front, striking WSW–ENE or W–E and dipping ~~either towards the orogen (synthetic faults)~~ towards either the orogen or the foreland (~~antithetic faults) (Figs. 8~~Fig. 6a, b~~, and Fig. 9~~). In cross-section, the majority of the faults appear planar and dip 75° to 85°, except for the ~~listric~~ faults Gartenberg S and Gartenberg N that have shallower dip angles of 60° to 65° (~~Figs. 4 and 6) already in the upper section of the reservoir, which further decrease with depth~~Fig. 3b, d).

With respect to their vertical extent and the stratigraphy they displace, the lower faults are subdivided, for descriptive purposes, into major and minor faults. The major faults offset crystalline basement and tip-out upward into Unit 4 (Rupelian) (e.g., Fault Gelting N, Fault NE), where the Rupelian reflections blanket the fault tips (Figs. ~~4, 9, 10~~3a–d, 5a). In contrast, the minor faults show no discernible offset of the basement and tip-out upward within either Unit 2 (Cretaceous) or lowermost Unit 4 (Rupelian). The tips of the minor faults that do not breach Unit 2 (Cretaceous) are overlain by monoclines (Fig. ~~4~~3b, d).

Two prominent graben structures in the NW and centre of the study area are defined by major conjugate faults (Fig. ~~7~~6a, b). The largest displacement across the NW graben is accommodated on the NW-dipping master fault, Fault Gelting N, with c. 150 m of throw at top Berriasian. Displacement along the northern flank of this graben is distributed across SE- and S-dipping, conjugate ~~and secondary, antithetic~~ faults. In contrast, the central graben switches its polarity ~~(i.e., controlling fault)~~ along strike from the northern boundary fault, Fault Gartenberg N, to the southern boundary fault, Fault Gartenberg S. In the western segment, ~~the~~ maximum displacement of c. 120 m is accrued at top Berriasian on the former fault, whereas in the eastern segment, the largest displacement of c. 150 m at top Berriasian is accrued on Fault Gartenberg S. ~~The switch of the graben polarity is also expressed by the presence of the rollover anticlines in the graben interior; in the west, there is a rollover anticline towards Fault Gartenberg N (Fig. 4), whereas in the east the rollover anticline is towards Fault Gartenberg S (Fig. 9).~~ ~~The~~ Displacement on the bounding faults of the central graben ~~have no displacement~~ at top Callovian are difficult to determine. It probably falls below the vertical resolution limit of 55 m at this depth. ~~The along-strike seismic section (Fig. 5) through the central graben clearly shows thinning of Unit 1 (Upper Jurassic) within the graben.~~

5.2.2 Upper fault array

The upper fault array exhibits reverse~~faulting geometries~~ /normal fault geometry in the central and northern parts of the study area — Cenozoic (CZ) reverse faults 1, 2, 3, and 4 (Figs. ~~7, 8~~4, 6d, f) and normal ~~faulting geometries~~ fault geometry in the southern part — Cenozoic (CZ) normal faults (Figs. ~~7, 8~~4, 6d). The upper faults strike approximately in the same direction as the lower faults~~, and show considerable lateral offset with respect to their lower counterparts~~ . In the map view, the traces of the upper faults at top Rupelian show considerable offset from the traces of the lower faults at top Berriasian (Fig. **??**6h). The lateral extent of the upper faults does not correlate with the lateral extent of the lower faults (Fig. **??**6h). Like the lower faults, the upper faults have alternating dip directions; they dip either to the S or to the N (Fig. ~~7, 8~~4, 6d, f)~~, often showing opposing dip with respect to each other~~. The dip angles of the CZ reverse faults range from 50° to 60°, whereas the CZ faults showing normal fault geometry dip steeper — 65° to 70°.

The upper faults offset the mechanically competent Unit 5 (Baustein beds) and die out upwards in Unit 6 (Chattian) and extend downwards into Unit 4 (Rupelian) (~~Figs. 4 and 6~~Fig. 3a–d), where the observation of internal deformation is hindered by the semi-transparent reflections. The CZ reverse faults have low throw magnitudes that do not exceed 50 m at both top Rupelian and top Baustein beds. In contrast, the CZ faults with normal fault geometry reach maximum throw values at top Rupelian that are twice that of the reverse faults (c. 100 m; Fig. ~~8~~6d).

5.2.3 Thrust faults

The normal faults of the upper fault array are overprinted by the extensive Geretsried Thrust that dips 20° to 35° to the S and has two branches. Its ~~stratigraphically higher upper branch thrust~~ upper branch dips parallel to the lower ~~master~~ thrust within Unit 6 (Chattian) (Fig. ~~10~~5a). Both thrust faults terminate with ramps within Unit 6 (Chattian) — no upper detachment is observed.

To understand the evolution of the thrust faults that dominate the deformation pattern of the Cenozoic sequence in the southern part of the study area, we investigated their geometries, up to the Kirchbichl Thrust, the frontal thrust of the Folded Molasse. The seismic profiles A and B (Figs. ~~10 and ??~~5a and 5b, resp.), depict the southward continuation of the Geretsried Thrust. ~~They also illustrate the overall tectonic style at the northern tip of the Alpine orogen, which is dominated by a simple overthrust (the Kirchbichl Thrust) with a minor triangle zone in its footwall. At the foot of the thrust, the Cenozoic sediments are tilted to the N to a varying extent, as shown in the profiles A and B.~~

In the western profile A~~(Fig. 10)~~, the Geretsried Thrust ~~emanates from~~ seems to be connected to a basal décollement below the carbonate platform, c. 4 km south of the study area~~, and~~ . It truncates both the Mesozoic and Cenozoic units over a distance of c. 7 km, dying out in the upper part of Unit 6 (Chattian). An upper thrust branches from the main Geretsried Thrust within Unit 4 (Rupelian), with a steeper dip (c. 45°) within Unit ~~5.~~ 5 (Baustein beds). The flat-ramp geometry of the Geretsried Thrust creates a distinct NNW-verging hanging-wall anticline — the Geretsried Fold. Where the Geretsried Thrust ~~steps over~~ cuts through the linkage zone, i.e., relay ramp, between the two CZ normal faults, the core of the Geretsried Fold is ~~extensively deformed by~~ deformed by two back-thrusts and a shallow-dipping reverse fault that accommodate shortening of Units 5 and 6 (~~Figs. 4, 6~~Fig. 3a–d). Here, the thrust dips steeper (c. 35°) ~~(Fig. ??)~~ and the fold core exhibits typical asymmetry, with a narrower forelimb and a broader, shallow-dipping backlimb.

In the eastern profile B~~(Fig. ??)~~, the Geretsried Thrust likewise ~~ramps up from the basement into the~~ truncates the carbonate platform, but terminates already within Unit ~~4.~~ 4 (Rupelian). There is no thrust-related folding above the Geretsried Thrust beyond Unit 4. ~~Notably in this profile , the Cenozoic Molasse sediments~~

The profiles A and B also illustrate the overall tectonic style at the northern edge of the Alpine orogen, which is dominated by a simple overthrust (the Kirchbichl Thrust). A notable feature that distinguishes the two profiles from each other is the geometry of the upper Cenozoic reflections, close to the Kirchbichl Thrust; in the profile A the reflections are sub-horizontal, whereas in the profile B they are tilted to the N~~to a much greater extent than in the western profile, where the Geretsried Thrustpropagated further into the foreland~~, showing increasing dip towards the Kirchbichl Thrust.

5.3 Structural analysis of selected faults

To infer the syn-depositional activity of the interpreted faults, we analysed thickness variations of the seismic-stratigraphic units using isochore maps (Fig. ~~??~~7). Unit 1 ~~in Figure ??adisplays no significant thickness variation across major faults that offset the basement.However, it~~ (Upper Jurassic) displays substantial thinning within the central graben (Figs. 3e–f and 7a). Such thickness reduction could be the result of sequential slip of the conjugate faults Gartenberg S and Gartenberg N that crosscut within Unit 1 and offset each other (Fig. 3b, d) (e.g., Ferrill et al., 2000, 2009; Budach et al., 2017). Unit 1 also shows slight thinning of hanging-wall blocks of minor faults that do not reach into the basement. Isochore map in Figure ~~??~~7b shows no consistent thickening of Unit 2 (Cretaceous) across all major faults. There are however local thickness variations in form of footwall thinning and hanging-wall thickening across Fault Gartenberg S, eastern segment of Fault NE and Fault Gartenberg N, and the central segment of Fault Gelting N. In the south, local depocentres are observed in Unit 2 that are not related to fault activity. Unit 3 (Priabonian) thickens only across Fault Gartenberg N (Fig. ~~??~~7c). In contrast to the underlying units,

the Rupelian ~~clays~~ clayey marl of Unit 4 (Rupelian) clearly exhibit a syn-kinematic nature, particularly where faults emerge from the carbonate platform (Fig. ~~??~~7d). This is especially evident within the central and the NE grabens, where the Rupelian strata is thicker than to the north or south of the graben-bounding faults. Furthermore, we observe onlapping of the Rupelian reflections onto the top Priabonian reflection in the easternmost margin of the graben (Fig. ~~5~~3e, f). In the ~~southeastern~~ southern part, there is a profound thickness decrease of Unit 4 associated with downthrow of the hanging-wall blocks of the upper CZ normal faults ~~(~~affecting the overlying Unit 5 (Baustein beds) (Fig. ~~??~~7d). Unit 5 displays no thickness variations across upper faults, except in the southeast, where it is thickened by displacement on the Geretsried Upper Thrust (Fig. ~~??~~7e). Although Unit 6 (Chattian) in Figure ~~??~~7f continuously thickens towards the S, it thins within the hanging-wall anticline (i.e., the Geretsried Fold).

~~Figures ??, ?? and ?? depict~~ Figure 8 depicts Allan maps and throw-depth diagrams of ~~Fault NE, Fault~~ faults NE, Gartenberg S, and ~~Fault~~ Gelting N, respectively, that are used to specify the temporal evolution of the lower faults. Fault NE is fully imaged by the seismic data. This allows us to document the geometry of its tip lines at the lateral terminations. The tip lines converge up- and down-dip from top Berriasian and must eventually meet within Unit 4 and the basement, correspondingly (Fig. ~~??~~8a). The largest throw is located at top Berriasian (c. 100 m, as shown in profile 3), from which it decreases both up- and downwards (Fig. ~~??b~~8a). The upward decrease of throw is gradual in profiles 1 and 2, whereas in profiles 3 and 4, throw minima are observed (Fig. ~~??b~~8a). These correspond to the local thinning and thickening of Unit 2 ~~(Turonian)~~ at the eastern segment of the fault plane (Fig. ~~??~~7b). Fault Gartenberg S has no detectable throw at top Callovian, so only three cut-off polygons are available for the throw analysis (Fig. ~~??a~~8b). Similar to Fault NE, the lateral extent of Fault Gartenberg S decreases up-dip and the fault throw is the largest at top Berriasian. All throw minima are located at top Turonian on *t*-*z* profiles (Fig. ~~??~~8b). For Fault Gelting N it is more difficult to establish a distinct trend of throw distribution (Fig. ~~??~~8c). This could be due to the overall poorer image quality at the fault region, which ~~introduced~~ introduces uncertainty in cut-off picking, especially at top Callovian. Generally, the throw on Fault Gelting N is distributed equally from top Callovian to top Priabonian, with a minor throw reduction at top Turonian (Fig. ~~??b~~8c). As shown in the *t*-*z* plot (Fig. ~~??b~~8c), the throw values vary mostly only by c. 25 m.

~~A~~ An Allan map of the ~~cut-off lines at top Baustein beds depicts the lateral distribution of throw on the Geretsried Thrust~~ Geretsried Thrust depicts the distribution of its throw at top Baustein beds (Fig. ~~??~~9). The thrust rapidly loses throw to the east: from c. 250 m in the westernmost extent of the survey area to the negative throw values of c. 50 m in the easternmost extent. The negative throw values are presumably the result of the residual slip on the pre-existing CZ normal faults that were not completely reversed. Similarly, the ~~the~~ upper branch of the Geretsried Thrust dies out to the east within the study area. The loss of displacement on the thrust faults is reflected by the eastward termination of the Geretsried Fold (Fig. ~~??~~6g). Due to poor resolution of the uppermost part of the seismic volume recognition of growth strata above the Geretsried Fold is not possible.

6 Discussion

The deformation pattern in our study area is characterised by two geometrically decoupled fault arrays, with both normal and reverse sense of slip~~and~~ , and the through-going ~~thrust faults~~Geretsried Thrust. Such a deformation pattern documents three distinct phases of faulting activity, which implies a paleostress change during the evolution of the foreland basin. In this section, we interpret our observations on reflection configuration, fault throw distribution, stratal thickness variations, and spatial relationships between faults to describe the temporal and spatial evolution of the faults in the Geretsried area. Furthermore, we discuss the governing factors on the evolution of the fault network that defined the present-day deformation pattern, such as evolving stress states, pre-existing deformation structures, and mechanical stratigraphy.

6.1 Temporal and spatial evolution of the fault network

Structural analysis suggests that the investigated fault network evolved in three phases: (1) normal faulting in the ~~early Rupelian~~Early Oligocene (Rupelian), (2) normal faulting in the ~~Chattian~~Late Oligocene (Chattian), and (3) reverse and thrust faulting in the mid-Miocene.

The first faulting phase occurred in the ~~early Rupelian~~Early Oligocene (Rupelian) and resulted in the formation of the lower fault array. Two lines of stratigraphic evidence provide time constraints for the ~~lower fault activity~~activity of the lower fault array; (1) substantial thickening of the syn-orogenic Rupelian strata across faults (Fig. ~~??~~7d), and (2) onlap and discordant patterns of the Rupelian reflections within the hanging-wall blocks (e.g., Fig. ~~5~~3e, f). Faulting activity ceased before the sedimentation of Rupelian was complete, as the fault tips are covered by the Rupelian reflections and there is no apparent offset at top Rupelian (Figs. ~~4, 6, and 10~~3a–d and 5a). These findings are in accordance with the works of Bachmann and Müller (1991) and Sissingh (1997), who report ~~Priabonian to Rupelian~~ Late Eocene to Early Oligocene syn-sedimentary faulting in the southern part of the GMB, based on the interpretation of regional seismic profiles.

The upper faults with reverse sense of slip most probably formed as normal faults, as suggested by their strike (i.e., WSW–ENE strike) and steep dips. The absence of geometrical coupling between the lower and upper faults and their overall distinct geometries (e.g., varying lengths, considerable ~~lateral~~ fault trace offset, opposite dip directions), indicate that the latter faults developed independently from the former faults, in the shallower Cenozoic level. We infer that they developed during the second faulting phase in the ~~Chattian~~Late Oligocene (Chattian). The evidence, such as (1) limited thickness variations across faults in the Baustein strata (Fig. ~~??~~7d), and (2) termination of the fault tips within the Chattian strata (~~Figs. 4 and 6~~Fig. 3a–d), shows that the upper faults initiated after the deposition of the Baustein beds (Unit 5), and were syn-sedimentary during deposition of the Chattian sandstones (Unit 6).

The third faulting phase is signified by the reverse reactivation of the upper normal faults, development of the Geretsried ~~thrust~~Thrust, and thrust-related folding in the mid-Miocene times. Due to the resolution limit in the upper part of the 3D seismic cube, it was impossible to recognise growth strata above the Geretsried Fold that could provide age constraints for the contractional deformation. However, we hypothesise that the Geretsried ~~thrust~~ Thrust was contemporaneous with ~~or succeeded~~ the frontal thrusts of the Folded Molasse, because it is rooted below the Folded Molasse and is thus kinematically related to

the frontal thrusts. ~~This implies a forward-propagating Alpine thrust system, which is most likely.~~ The documented age of the growth strata within the tilted footwall of the Kirchbichl Thrust indicates that the contractional deformation started in the ~~Badenian~~ late Middle Miocene (Serravalian) (Unger, 1989; Ortner et al., 2015).

6.2 ~~Controlling factors on fault~~ Stress field evolution~~in the southern GMB~~

6.2.1 ~~Stress field evolution~~

The temporal and spatial evolution of the deformation structures in the Geretsried area ~~are~~ was primarily controlled by the evolving stress states in the foreland foredeep. Each of the identified faulting phases marks ~~the~~ changes in the ~~regional stress field triggered by the migration of the forebulge and foredeep across the study area , as the Alpine front propagated northwards~~stress field at the study area related to the northward propagation of the Alpine orogen.

The ~~first faulting phase was triggered by the~~ longitudinal strike of the lower and upper faults, with respect to the Alpine orogenic front, implies that they formed due to the flexure-induced ~~extensional stress field~~deformation on the foredeep slope. It has been ~~recognised~~ recognized that during foreland flexuring, the upper ~~and lower parts~~ part of the bending plate ~~experience extensionand compression, respectively, whereas~~ experiences extension, the lower part — compression, and a central horizon is neutral (Turcotte and Schubert, 1999; Price and Cosgrove, 1990). Within the region of maximum flexure ~~,~~ (i.e., foreland forebulge), elastic bending facilitates an extensional stress field with ~~the negative~~ an effective minimum stress oriented perpendicular to the trend of the foredeep ~~(Bradley and Kidd, 1991; Bachmann and Müller, 1992; Londoño and Lorenzo, 2004; Langhi et al., 201~~ ~~.~~(Bradley and Kidd, 1991; Bachmann and Müller, 1992; Londoño and Lorenzo, 2004; Langhi et al., 2011). As the syn-orogenic load within the foredeep increases towards the orogen, the sub-vertical maximum principle stress increases as well. Consequently, normal faults form in a basinward position with respect to the region of maximum flexure, striking parallel to the ~~trend of the foredeep . The WSW–ENE and W–E strike of the lower faults is consistent with the transient extensional stress field that must have existed in the Molasse Basin due to the northward propagation of the flexural front. We thus infer that the lower fault activity initiated as the forebulge,~~ foredeep axis (Tavani et al., 2015).

The first faulting phase initiated in the Early Oligocene (early Rupelian), as evidenced from the seismic data. At this time, the GMB was characterised by a limited sediment supply (Zweigel et al., 1998). Hence, we imply that the magnitude of the sub-vertical stress was low as the lower fault array formed. Presumably, the lower normal faults occurred in the distal foredeep, close to the region of maximum flexure, ~~reached the Geretsried area in the early Rupelian. With the ongoing propagation of the Alpine thrusts onto the foreland, the effective minimum stress eventually attained positive values, which resulted~~ where the magnitude of the horizontal compression was still small enough for the differential stress to cause normal faulting. As the Alpine orogen moved forward, the magnitude of the horizontal stress component increased, resulting in termination of normal faulting in the late Rupelian.

~~Renewed tectonic activity in the foreland basin, signified by the development of the upper normal faults within the Cenozoic Molasse sequence, indicates that a normal faulting stress regime was established at this stratigraphic level. The longitudinal strike of the upper faults implies that the established stress regime was caused by the same tectonics that triggered lower~~

faulting — the Cenozoic foreland flexure. By the Chattian times, the foreland foredeep approached the study area, as is evident from the southward thickness increase of Unit 6 The second faulting phase occurred in the Late Oligocene (Chattian)(Fig. ??f). This resulted in the onset of rapid sedimentation , as confirmed by the sequence-stratigraphic investigations (Jin et al., 1995; Zweigel et al., 1998) and the studies on pressure distribution (Müller et al., 1988; Müller and Nieberding, 1996) in the southern part of the GMB. Increasing sedimentary load towards the orogen produced an increase in . Zweigel et al. (1998) document a drastic increase of sedimentation rates at this time due to the increase in the topographic relief in the Alpine orogen. A rapid thickening of the sedimentary load must have resulted in an increase of the vertical stress magnitude (Drews et al., 2018) and therefore favoured that eventually exceeded horizontal compression, resulting in renewed normal faulting. The existence of a sub-vertical maximum stress in the Late Oligocene—Early Miocene is also implied from the build-up of overpressure in the Rupelian sequence that is related to high sedimentation rates during this time (Müller et al., 1988; Müller and Nieberding, 1996) .

While the increase of the vertical component of the stress field triggers normal faultingtriggered activation of the upper normal faults, the vertical gradient of the horizontal component, oriented perpendicular to the trend of the foredeep, governs must have governed the position of fault initiation. Due to the ongoing flexuring in the Chattian, the horizontal stress magnitude within the foredeep is expected to be smaller at shallower stratigraphic levels and conversely larger at deeper stratigraphic levels. The numerical model of stress in the Molasse Basin by von Hartmann et al. (2016) confirms the existence of the vertical stress gradients within the basin fill during the Cenozoic flexuringflexure. We therefore explain the independent development of the upper fault array in the shallower Cenozoic by lower magnitudes of the horizontal stress component that existed at this interval and acted perpendicular to the planes of the longitudinal faults. The horizontal stress component must have been the least principal stress for the normal faulting to initiate.

Reverse reactivation of the upper normal faults, thrusting and folding deformation during the third faulting phase point to a stress regime, in which the magnitude of the horizontal stress component, oriented parallel to the shortening direction, exceeded the magnitude of the vertical stress component. Such stress field configuration must have been established in the mid-Miocene as the Alpine thrust wedge approached the study area. The N–S directed shortening must have been was first accommodated by the reverse reactivation of the longitudinal upper normal faults due to their inherited low-cohesion and favourable orientation, and then eventually by the development of new thrusts.

6.2.1 Pre-existing structures

6.3 Pre-existing structures

Inherited deformation structures have been recognised as influencing to influence structural style, i.e., kinematic and geometrical interaction between faults in the foreland settings (e.g., Butler, 1989; Scisciani et al., 2001; Bry et al., 2004; Calamita et al., 2012; Tavani et al., 2015). In this subsection, we attempt to shed light on the following two questions:

1. Did any the lower fault array develop from the pre-existing of the lower faults develop from inherited pre-orogenic faults?

2. What is the kinematic relationship between the Geretsried Thrust and directly underlying faults with normal fault geometries?

~~**Pre-orogenic inheritance: Did any the lower fault array develop from the pre-existing pre-orogenic faults?**~~

6.3.1 Pre-orogenic inheritance: Did any of the lower faults develop from inherited pre-orogenic faults?

Pre-orogenic normal faults that are oriented sub-parallel to the developing fold-and-thrust belt are the favourable structures to be extensionally reactivated during ~~the~~ foreland flexuring (Butler, 1989; Bry et al., 2004; Tavani et al., 2015, 2018). In the ~~Western~~ Swiss Molasse Basin, the basement structures are interpreted to act as the loci of the flexure-induced normal faulting (J. Mosar, personal communication, 2018). In the ~~Eastern Molasse Basin~~GMB, Budach et al. (2017) and Mraz et al. (2018) report reactivation of the Mesozoic normal faults during the Cenozoic flexuring. Based on ~~the~~ our structural evidence, we discuss in this section whether ~~the analyzed~~ in this study the analysed faults of the lower fault array had a pre-orogenic ~~activity~~origin.

The results of throw distribution on the lower faults show three major trends from top Berriasian down to top Callovian (i.e., near top basement): (i) throw diminishes (Fault NE; Fig. ~~??~~8a), (ii) throw decreases nearly to zero (Faults Gartenberg S and Gartenberg N; Figs. ~~4, 6 and ??~~3a–d and 8b), and (iii) throw remains constant (Fault Gelting N; Fig. ~~??).~~ 8c). The former two cases suggest that the faults propagated into the basement from the shallower stratigraphic unit. The near-elliptical tip lines of faults NE and Gartenberg S imply an initially elliptical slip distribution on these faults (Barnett et al., 1987). Such slip distribution is characteristic of blind fault growth by radial propagation, whereby the site of fault nucleation typically corresponds to the region of maximum displacement (Watterson, 1986; Barnett et al., 1987; Walsh and Watterson, 1987; Baudon and Cartwright, 2008a, b). The throw distribution on the faults NE, Gartenberg S and Gartenberg N shows that the maximum displacement could occur between top Callovian and top Berriasian, suggesting that these faults nucleated within the carbonate platform and were not rooted in the basement. Fault Gelting N is the only fault in our study area that could have originated within the pre-fractured basement, since it shows no decrease in displacement with depth, down to top Callovian.

A substantial upward decrease in fault throw from top Berriasian to top Turonian, as is observed in the study area on faults NE (Fig. ~~??~~8a) and Gartenberg S (Fig. ~~??~~8b), has been also reported 25 km to the NNE and 55 km to the W, in the Unterhaching and Mauerstetten geothermal sites, respectively (Budach et al., 2017; Mraz et al., 2018). Such high displacement ~~gradient~~ gradients can indicate either (1) fault interaction with the free surface, i.e., syn-sedimentary activity, if the displacement gradient increase coincides with the stratigraphic expansion of the displaced units across faults or (2) propagation across a mechanical barrier, if there is no stratigraphic expansion (Baudon and Cartwright, 2008a). The former case is confirmed ~~in~~ to the Unterhaching and Mauerstetten areas, where ~~, as Budach et al. (2017) and Mraz et al. (2018) infer, faults had a~~ it is inferred that the faults were syn-sedimentary ~~activity~~ in the Mesozoic. In contrast, in ~~this~~ the Geretsried area, we do not observe stratigraphic expansion of the ~~Turonian Unit 2~~ Mesozoic units across the analysed faults. ~~Even though there is~~ The local thickening of ~~the Turonian~~ Unit 2 in the hanging-wall ~~, it~~ is accompanied by ~~the thinning of the same unit~~ thinning in the footwall. This ~~suggests ductile deformation of the Turonian sediments acted as a barrier~~ indicates ductile deformation within Unit 2 in response to fault

propagation. Based on this evidence, we rule out the possibility ~~of the Mesozoic faults in the Geretsried area having attracted flexural-induced~~ that the identified faults originated in the Mesozoic and accommodated further extension in the Cenozoic.

~~**Early-orogenic inheritance: What is the kinematic relationship between the Geretsried Thrust and directly underlying faults with normal fault geometries?**~~

6.3.2 Early-orogenic inheritance: What is the kinematic relationship between the Geretsried Thrust and directly underlying faults with normal fault geometries?

Early-orogenic inheritance plays a significant role in the spatial evolution of the contractional deformation. A characteristic geometrical relationship between the Geretsried Thrust and the directly underlying normal faults suggests a possible kinematic interaction between them in the past. Such overprinting relationships between flexure-induced normal faults and later developed contractional structures have been recognised in foreland basins at the toe of the orogenic wedges elsewhere ~~(e. g., Scisciani et al.~~(e.g., Scisciani et al., 2001; Bry et al., 2004; Calamita et al., 2012). In the GMB, c. 25 km east of our study area, Müller (1975/1976) interpreted a frontal thrust structure with a similar geometry to the Geretsried Thrust that also truncates an early-orogenic normal fault. The fact that the Geretsried Thrust dies out rapidly to the east suggests that the thrust interpreted by Müller (1975/1976) must have formed separately from the Geretsried Thrust.

According to Tavani et al. (2015), ~~2001, Bry et al. , 2004, Calamita et al. , 2012). According to Tavani et al. (2015),~~ thrust fault nucleation and propagation may occur even in a strike-slip faulting stress regime, facilitated by the reverse reactivation of pre-existing normal faults that strike perpendicular to the shortening direction. These authors argue that the strain at the tips of positively inverted faults or in the overstep areas between them produces local contractional ~~areas~~ stress field and causes re-orientation of the maximum principal stress axis until it reaches favourable angle with the bedding, eventually resulting in a slip. Such a local perturbation of the stress field at the tips of the inverted faults may favour nucleation and propagation of an about 30° dipping, new fault segment that further develops into a thrust fault. It is likely that the Geretsried ~~thrust~~ Thrust developed according to this scenario. An approximately 30°–35° dipping thrust ramp ~~(Fig. ??)~~ must have initiated in the step-over area between the CZ normal faults, ~~that~~ as they were undergoing reverse reactivation, and from there propagated both upwards and downwards. It eventually reached beneath the Upper Jurassic carbonate platform and connected to a basal décollement beneath it. The prominent Geretsried Fold above the thrust ramp most probably developed due to the buttressing of the thrust displacements against the pre-existing normal faults (e.g., Butler, 1989; Scisciani et al., 2001).

The early-orogenic inheritance ~~must have also~~ could have locally influenced the style of deformation in the transition zone between the Foreland Molasse and the Folded Molasse~~, immediately south of the Geretsried area.The northern extent of the Geretsried Fold within the survey area coincides with the northern limit of~~ . Our interpretation of the profiles A and B (Figs. 5a and 5b, resp.) confirms already existing interpretations, which characterise the Folded Molasse front in the study area by a simple overthrust without a major triangle zone at depth (e.g., Schwerd and Thomas, 2003; Thomas et al., 2006; Ortner et al., 2015) . Despite the absence of a large triangle zone, which, as has been documented, controls the width of the tilted Molasse (e.g., Müller et al., 1988), the upper Cenozoic reflections are tilted in the profile B. Such reflection pattern must represent

true tilting of the beds and is unlikely to be an imaging artefact, i.e., velocity pull-up, as in such a case similar tilting would be also observed in the profile A. Presumably, the area increase between the tilted upper beds and the sub-horizontal lower beds in the ~~tilted Molasse on the tectonic map of the Folded Molasse by Ortner et al. (2015) (Fig. 1b).The seismic profile A in Figure 10 clearly shows that the extent of~~ profile B was produced by a diffuse, i.e., distributed, sub-seismic strain. In contrast, in the profile A, no sub-seismic deformation of such a scale took place, as the tilted Molasse ~~south of the Geretsried area is much narrower than shown by Ortner et al. (2015). The area~~ is absent. The northern limit of the tilted Molasse ~~broadens significantly to the east, while the~~ on the tectonic map of the Folded Molasse by Ortner et al. (2015) within the study area is in fact the northern extent of the Geretsried ~~Thrust decreases~~ Fold (Fig. ~~??~~1b). We postulate that ~~the varying amplitude of the tilted zone from west to east must be controlled by the occurrence of early-orogenic normal faults that facilitate thrusting. In the Geretsried area and south of it, the Geretsried Thrust~~accommodated shortening ~~and thereby prevented large-scale folding~~ in the study area the shortening was primarily accommodated by the Geretsried Thrust, which prevented large sub-seismic strain in front of the ~~propagating Alpine thrust sheets. In contrast, to~~ thrusts of the Folded Molasse. To the east, in the absence of inherited extensional structures and therefore thrust faulting, the shortening was accommodated by distributed sub-seismic deformation and consequent amplification of the tilted zone ~~at the foot~~ in front of the Kirchbichl Thrust.

6.3.3 ~~Mechanical stratigraphy~~

6.4 Mechanical stratigraphy

The fault growth in the southern GMB is influenced by the different mechanical behavior of rock layers. We show in this subsection that mechanically incompetent layers within the Meso-Cenozoic sequence act as fault propagation barriers, resulting in variations in fault plane geometries, development of extensional forced folding and decoupling of the lower and upper fault arrays.

~~Growth of the lower faults~~

6.4.1 Growth of the lower faults

As we postulated in the previous subsection, the majority of the lower faults nucleated in the carbonate platform and grew by radial propagation. The down-dip propagation of individual faults could have been affected by the mechanical behaviour of the Dogger shales/marls (below top Callovian). For instance, ~~the occurrence of the rollover structures within the central graben suggests that graben-bounding faults , Gartenberg S and Gartenberg N, propagated down into the detachment beneath the carbonate platform that accommodated flexure-induced extension~~substantial decrease in fault throw on faults Gartenberg N and Gartenberg S could indicate that at this boundary faults intersect a less competent layer that accommodates deformation by distributed deformation. Up-dip propagation was restricted by the Turonian layer of Unit 2. We postulate that the aforementioned high displacement gradient for faults NE and Gartenberg S (~~Figs.15 and 16~~Fig. 8a, b) resulted from the additional slip that accumulated at the mechanical boundary for the faults to propagate through the barrier (e.g., Wilkins and Gross, 2002;

Baudon and Cartwright, 2008a)~~, resulting in the aforementioned high displacement gradient for faults NE and Gartenberg S (Figs. ?? and ??).~~ .

~~We postulate that the aforementioned high displacement gradient for faults NE and Gartenberg S (Figs. 15 and 16) resulted from the additional slip that accumulated at the mechanical boundary for the faults to propagate through the barrier (e.g., Wilkins and Gross, 2002; Baudon and Cartwright, 2008a)~~

Two features point to a restricting behaviour of the Turonian marls: 1) extensional forced folding above tips of normal faults and 2) the staircase geometry of Fault Gartenberg S. Mechanically incompetent layers accommodate pre-failure strain by distributed ductile deformation, which causes extensional forced folding and thinning of the incompetent layer at the footwall (Walsh and Watterson, 1987; Withjack et al., 1990; Childs et al., 1996; Withjack and Callaway, 2000; Schöpfer et al., 2006; Ferrill et al., 2012). In our study area, this kind of deformation is especially evident above the minor lower faults (~~Figs. 4 and 6~~Fig. 3a–d). Here, unbreached monoclines indicate that fault propagation was arrested by the clay-rich Turonian layer, hindering the faults to interact with the free surface. Hanging-walls of the major lower faults that managed to propagate across the Turonian barrier locally exhibit normal drag, which presumably formed as precursory monoclines ~~,~~ were breached (Fig. ~~6~~3c, d). Extensional forced folding is also confirmed by local thinning and thickening of the Turonian ~~marls (Unit 2)~~ clayey marls across the faults (Fig. ~~??~~7b).

The staircase geometry of Fault Gartenberg S (Fig. ~~6~~3c, d) indicates fault growth by vertical segment linkage in the presence of a mechanical barrier (Childs et al., 1996; Walsh et al., 2003; Schöpfer et al., 2006). According to the coherent fault model by Walsh et al. (2003) and discrete element models of Schöpfer et al. (2006), kinematically connected fault segments first initiate in strong layers, whereas weak layers deform by ductile flow. Increasing strain results in shear failure of the weak layers and eventual linkage of the fault segments. The resulting through-going fault thus attains a staircase geometry. The shallower dip of Fault Gartenberg S within the Turonian marls corresponds to the throw minimum at top Turonian that separates two throw maxima at top Berriasian and top Priabonian (Fig. ~~??~~8b). We propose that ductile deformation of ~~Unit 2~~ the Turonian clayey marls promoted vertical fault segmentation of Fault Gartenberg S, whereby an upper fault segment formed in the more competent Unit 3 (Priabonian) and linked downwards with the lower segment of Gartenberg S within Unit ~~2.~~ 2 (Cretaceous).

Having considered the impact of mechanical stratigraphy, we propose the following growth history of the lower faults, which is illustrated in Figure ~~??~~10:

1. Lower normal faults initiated within the carbonate platform and possibly, in case of Fault Gelting N, in the basement.

2. The faults propagated radially from the point of nucleation as blind faults. The up-dip propagation was inhibited by the Turonian marls, resulting in monoclinal folding of the overlying layers. Minor faults were arrested by the mechanical barrier, whereas major faults continued to propagate across it, in individual cases, by vertical segment linkage.

3. As fault slip continued, major faults breached the monoclines above them and reached the free surface during sedimentation of the Rupelian ~~clays~~clayey marl, thereby switching from being blind to ~~syn-sedimentary~~emergent. Eventually, faulting ceased and the stagnant fault tips were buried by the later Rupelian sediments.

~~Decoupled evolution of the fault network~~

6.4.2 Decoupled evolution of the fault network

As we have put forward in the previous subsection on stress field evolution, the stress conditions in the Chattian were favourable for the independent development of the upper faults in the Cenozoic interval. Faults are expected to nucleate first in the most competent unit of the multi-layered Cenozoic sequence, since the less competent units are able to accommodate greater pre-failure strain (Eisenstadt and De Paor, 1987; Ferrill et al., 2017). The fault geometries suggest that the upper faults nucleated indeed within the competent Baustein beds, and grew by both up- and downward propagation. Such isolated fault growth within the Cenozoic Molasse is also reported c. 35 km E of our study area by von Hartmann et al. (2016), where the authors observe decrease in throw from central to outermost portions of the Cenozoic faults, both up- and down-dip.

As the upper faults propagated downward into the incompetent Unit 4 (Rupelian), they failed to connect with the lower faults by incidental dip linkage (e.g., Baudon and Cartwright, 2008c; Langhi et al., 2011). They flattened out within the Rupelian sediments, which are expected to have a lower angle of internal friction and ~~act as a detachment horizon~~ contain detachment horizons (Müller et al., 1988; Ortner et al., 2015). Although the observation of fault geometry within the Rupelian sequence is limited by its semi-transparent and non-coherent reflection configuration, the listric nature of the CZ normal faults ~~could~~ can be inferred from the thinning of Unit 4 (Rupelian) across these faults (Fig. ~~??~~7d).

At the same time, it is unlikely that the lower faults accommodated Chattian deformation by reactivation and upward propagation. We do not observe monoclinal folding within the mechanically weak Rupelian strata that would have developed if the lower faults had propagated across it (Schöpfer et al., 2006). We postulate that the upward propagation of the lower faults were inhibited due to the mechanical behaviour of ~~Rupelian clays~~ the Rupelian clayey marls that acted as a propagation barrier. In the latter case, the extensional strain could be accommodated by ductile, i.e., distributed, sub-seismic deformation within the Rupelian Unit 4. We conclude that the fault evolution in the presence of a thick mechanical barrier resulted in a decoupled structural style, as has been previously reported for the geometrically decoupled fault systems by Ferrill et al. (2007), Langhi et al. (2011), Lewis et al. (2013), and Deckers (2005).

7 Conclusions

We used 3D seismic data from the Geretsried area to analyse the structure and evolution of the fault network proximal to the European Alpine front. Structural analysis reveals that the fault network developed in three syn-orogenic deformation phases: (i) lower normal faulting in the ~~Rupelian~~Early Oligocene, (ii) upper normal faulting in the ~~Chattian~~Late Oligocene, and (iii) reverse and thrust faulting in the mid-Miocene. We demonstrate that these temporal phases correlate with the evolution of the stress field as the Alpine orogen moved forward. While the tectonic stresses are responsible for fault initiation, local stress 'modifiers', such as pre-existing structures and mechanical stratigraphy, govern the location of fault nucleation and its further spatial development.

A key observation of this study is that the lower and upper fault arrays developed independently, both temporally and spatially, with nucleation loci in the Upper Jurassic carbonate platform for the former fault array and in the Baustein beds for the latter. Vertical gradients of the flexural stresses pre-defined decoupled initiation of the upper faults with respect to the lower faults, whereas the mechanically incompetent Rupelian ~~clays~~ clayey marls inhibited further geometrical connection of the two fault arrays. The decoupled style of fault evolution has implications for geothermal exploration in the GMB, since we expect the isolated lower faults to develop less interconnected fractures and be more prone to healing by secondary mineralisation than through-going faults with a prolonged activity, which are observed elsewhere in the basin. In this respect, further investigations are required to establish correlation between the decoupled faulting style and the mechanical behaviour of the Rupelian ~~clays~~clayey marls.

Furthermore, ~~seismic interpretation documents~~ we document kinematic interaction between the upper normal faults and ~~large-scale~~ frontal thrusts. In particular, we postulate that the reactivation of CZ normal faults facilitated the initiation of the Geretsried ~~thrust~~Thrust, thereby preventing ~~a large accumulation of~~ accumulation of distributed sub-seismic strain at the ~~foot~~ front of the Folded Molasse. We therefore emphasise the importance of the early-orogenic structures on the style of contractional deformation in the transition zone between the Foreland and the Folded Molasse.

Data availability. The seismic data is not publicly accessible. The results of the seismic model are presented in the article. Detailed results can be provided by the first author on request.

Author contributions. VS designed the study, carried out the seismic interpretation and 3D structural modelling, wrote the manuscript, and prepared the figures. DT participated in analyzing the structural results and in the writing of the manuscript. HH contributed in interpreting the seismic data and drafting the manuscript. IM initiated the study. All authors commented, read, and approved the final manuscript.

Competing interests. No competing interests are present.

Acknowledgements. This work was carried out as part of the joint research project 'Play Type', financed by the German Ministry for Economic Affairs and Energy (FN: 0324210A). We thank Enex Power Germany GmbH and Wintershall Dea GmbH for access to seismic and well data and permission to publish images from these data. Seismic data acquisition and processing was carried out by DMT GmbH. We also thank ~~reviewers~~ Stefano Tavani and Hugo Ortner for their thorough reviews, which helped to improve this article. Jonas Kley, Jennifer Ziesch, Sonja Wadas, and Tom Schintgen are thanked for their useful comments on the manuscript.

References

Agemar, T., Alten, J., Ganz, B., Kuder, J., Kühne, K., Schumacher, S., and Schulz, R.: The geothermal information system for Germany — GeotIS, Z. Dtsch. Ges. Geowiss., 165(2), 129–144, https://doi.org/10.1127/1860-1804/2014/0060, 2014.

Allan, U. S.: Model for hydrocarbon migration and entrapment within faulted structures, AAPG Bull., 73(7), 803–811, https://doi.org/10.1306/44B4A271-170A-11D7-8645000102C1865D, 1989.

Allen, P. A., Crampton, S. L., and Sinclair, H. D.: The inception and early evolution of the North Alpine Foreland Basin, Switzerland, Basin Res., 3(3), 143–163, https://doi.org/10.1111/j.1365-2117.1991.tb00124.x, 1991.

Bachmann, G. H., Dohr, G., and Müller, M.: Exploration in a classic thrust belt and its foreland, Bavarian Alps, Germany, AAPG Bull., 66(12), 2529–2542, https://doi.org/10.1306/03B5AC69-16D1-11D7-8645000102C1865D, 1982.

Bachmann, G. H., Müller, M., and Weggen, K.: Evolution of the Molasse Basin (Germany, Switzerland), Tectonophysics, 137, 77–92, https://doi.org/10.1016/0040-1951(87)90315-5, 1987.

Bachmann, G. H., and Müller, M.: The Molasse Basin, Germany: evolution of a classic petroliferous foreland basin, in: Generation, Accumulation and Production of Europe's Hydrocarbons, edited by: Spencer, A. M. et al., Spec. Publ. Eur. Assoc. Petrol. Geoscien, No. 1, 263–276, 1991.

Bachmann, G. H., and Müller, M.: Sedimentary and structural evolution of the German Molasse Basin, Eclogae Geol. Helv., 85(3), 519–530, 1992.

Barnett, J. A. M., Mortimer, J., Rippon, J. H., Walsh, J. J. and Watterson, J.: Displacement geometry in the volume containing a single normal fault, AAPG Bull., 71(8), 925–937, https://doi.org/10.1306/948878ED-1704-11D7-8645000102C1865D, 1987.

Baudon, C., and Cartwright, J. A.: 3D seismic characterisation of an array of blind normal faults in the Levant Basin, Eastern Mediterranean, Journal of Structural Geology, 30, 746–760, https://doi.org/10.1016/j.jsg.2007.12.008, 2008a.

Baudon, C., and Cartwright, J.: Early stage evolution of growth faults: 3D seismic insights from the Levant Basin, Eastern Mediterranean, Journal of Structural Geology, 30, 888–898, https://doi.org/10.1016/j.jsg.2008.02.019, 2008b.

Baudon, C., and Cartwright, J.: The kinematics of reactivation of normal faults using high resolution throw mapping, Journal of Structural Geology, 30, 1072–1084, https://doi.org/10.1016/j.jsg.2008.04.008, 2008c.

Bradley, D. C., and Kidd, W. S. F.: Flexural extension of the upper continental crust in collisional foredeeps, Bull. Geol. Soc. Am., 103, 1416–1438, https://doi.org/10.1130/0016-7606(1991)103<1416:FEOTUC>2.3.CO;2, 1991.

Bry, M., White, N., Singh, S., England, R., and Trowell, C.: Anatomy and formation of oblique continental collision: South Falkland basin, Tectonics, 23, TC4011, https://doi.org/10.1029/2002TC001482, 2004.

Budach, I., Moeck, I., Lüschen, E., and Wolfgramm, M.: Temporal evolution of fault systems in the Upper Jurassic of the Central German Molasse Basin: case study Unterhaching, Int. J. Earth Sci. (Geol. Rundsch.), 107, 635–654, https://doi.org/10.1007/s00531-017-1518-1, 2017.

Butler, R. W. H.: The influence of pre-existing basin structure on thrust system evolution in the Western Alps, Geological Society, London, Special Publications, 44, 105–122, https://doi.org/10.1144/GSL.SP.1989.044.01.07, 1989.

Cartwright, J. A., Bouroullec, R., James, D., and Johnson, H. D.: Polycyclic motion history of some Gulf Coast growth faults from high-resolution displacement analysis, Geology, 26(9), 819–822, https://doi.org/10.1130/0091-7613(1998)026<0819:PMHOSG>2.3.CO;2, 1998.

Calamita, F., Pace, P., and Satolli, S.: Coexistence of fault-propagation and fault-bend folding in curve-shaped foreland fold-and-thrust belts: Examples from the Northern Apennines (Italy), Terra Nova, 24, 396–406, https://doi.org/10.1111/j.1365-3121.2012.01079.x, 2012.

Childs, C., Nicol, A., Walsh, J. J., and Watterson, J.: Growth of vertically segmented normal faults, ~~J. Struct. Geol.~~Journal of Structural Geology, 18(12), 1389–1397, https://doi.org/10.1016/S0191-8141(96)00060-0, 1996.

DeCelles, P. G. and Giles, K. A.: Foreland basin systems, Basin Res., 8, 105–123, https://doi.org/10.1046/j.1365-2117.1996.01491.x, 1996.

Deckers, J.: Decoupled extensional faulting and forced folding in the southern part of the Roer Valley Graben, Belgium, Journal of Structural Geology, 81, 125–134, https://doi.org/10.1016/j.jsg.2015.08.007, 2015.

Diem, B.: Die Untere Meeresmolasse zwischen Saane (Westschweiz) und der Ammer (Oberbayern), Ecl. Geol. Helv., 79, 493–559, 1986.

Drews, M. C., Bauer, W., Caracciolo, L., and Stollhofen H.: Disequilibrium compaction overpressure in shales of the Bavarian Foreland Molasse Basin: Results and geographical distribution from velocity-based analyses, Marine and Petroleum Geology, 24, 37–50, https://doi.org/10.1016/j.marpetgeo.2018.02.017, 2018.

Eisenstadt, E., and De Paor, D. G.: Alternative model of thrust-fault propagation, Geology, 15(7), 630–633, https://doi.org/10.1130/0091-7613(1987)15<630:AMOTP>2.0.CO;2, 1987.

Freudenberger, W., and Schwerd, K.: Erläuterungen zur geologischen Karte von Bayern 1:500 000. Bayerisches Geologisches Landesamt, München, 329 pp., 1996.

Ferrill, D. A., Morris, A. P., Stamatakos, J. A., and Sims, D.: Crossing conjugate normal faults, AAPG Bull., 84(10), 1543—1559, https://doi.org/doi.org/10.1306/8626BEF7-173B-11D7-8645000102C1865D, 2000.

Ferrill, D. A., Morris, A. P., and Smart, K. J.: Stratigraphic control on Extensional fault propagation folding: Big Brushy Canyon monocline, Sierra del Carmen, Texas, Geol. Soc. Lond. Spec. Pub., 292, 203–217, https://doi.org/doi.org/10.1144/SP292.12, 2007.

Ferrill, D. A., Morris, A. P., McGinnis, R. N.: Crossing conjugate normal faults in field exposures and seismic data, AAPG Bull., 93(11), 1471—1488, https://doi.org/doi.org/10.1306/06250909039, 2009.

Ferrill, D. A., Morris, A. P., and McGinnis, R. N.: Extensional fault-propagation folding in mechanically layered rocks: The case against the frictional drag mechanism, Tectonophysics, 576–577, 78–85, https://doi.org/10.1016/j.tecto.2012.05.023, 2012.

Ferrill, D. A., Morris, A. P., McGinnis, R. N., Smart, K. J., Wigginton, S. S., and Hill, N. J.: Mechanical stratigraphy and normal faulting, Journal of Structural Geology, 94, 275–302, https://doi.org/10.1016/j.jsg.2016.11.010, 2017.

Fischer, W.: Stratigraphische und tektonische Beobachtungen im Gebiet der Mumauer Mulde und Steineberg Mulde (Oberbayern, Allgäu und Vorarlberg), Bull. Ver. Schweiz. Petrol.-Geol. u.-Ing., 27, 39–57, 1960.

Frisch, W.: Tectonic progradation and plate tectonic evolution of the Alps, Tectonophysics, 69, 121–139, https://doi.org/10.1016/0040-1951(79)90155-0, 1979.

GeoMol Team: GeoMol — Assessing subsurface potentials of the Alpine Foreland Basins for sustainable planning and use of natural resources, Project Report, LfU, Augsburg, 188 pp., 2005.

Jackson, C. A.-L., and Larsen, E.: Temporal and spatial development of a gravity-driven normal fault array: Middle–Upper Jurassic, South Viking Graben, northern North Sea, Journal of Structural Geology, 31, 388–402, https://doi.org/10.1016/j.jsg.2009.01.007, 2009.

Jackson, C. A.-L., and Rotevatn, A.: 3D seismic analysis of the structure and evolution of a salt-influenced normal fault zone: a test of competing fault growth models. Journal of Structural Geology, 54, 215–234, https://doi.org/10.1016/j.jsg.2013.06.012, 2013.

Jin, J., Aigner, T., Luterbacher, H. P., Bachmann, G. H., and Müller, M.: Sequence stratigraphy and depositional history in the south-eastern German Molasse Basin, Mar. Pet. Geol., 12, 929–940, https://doi.org/10.1016/0264-8172(95)98856-Z, 1995.

Kley, J., and Voigt, T.: Late Cretaceous intraplate thrusting in central Europe: Effect of Africa-Iberia-Europe convergence, not Alpine collision, Geology, 36(11), 839–842, https://doi.org/10.1130/G24930A.1, 2015.

Kuhlemann, J., and Kempf, O.: Post-Eocene evolution of the North Alpine Foreland Basin and its response Alpine tectonics, Sedimentary Geology, 152, 45–78, https://doi.org/10.1016/S0037-0738(01)00285-8, 2002.

Langhi, L., Ciftci, N. B., and Borel, G. D.: Impact of lithospheric flexure on the evolution of shallow faults in the Timor foreland system, Marine Geology, 284, 40–54, https://doi.org/10.1016/j.margeo.2011.03.007, 2011.

Lemcke, K.: Zur nachpermischen Geschichte des nördlichen Alpenvorlandes, Geologica Bavarica, 69, 5–48, 1973.

Lemcke, K.: Das heutige geologische Bild des deutschen Alpenvorlandes nach drei Jahrzehntehn Öl- und Gasexploration, Eclogae Geologicae Helveriae, 74, 1–18, https://doi.org/10.5169/seals-165086, 1981.

Lemcke, K.: Geologie von Bayern, Bd. 1, Das bayerische Alpenvorland vor der Eiszeit, E. Schweizerbart'sche Verlagsbuchhandlung, Stuttgart, 1988.

Lewis, M. M., Jackson, C. A. L., and Gawthorpe, R. L.: Salt-influenced normal fault growth and forced folding: the Stavanger fault system, North Sea, Journal of Structural Geology, 54, 156–173, https://doi.org/10.1016/j.jsg.2013.07.015, 2013.

Londoño, J., and Lorenzo, J. M.: Geodynamics of continental plate collision during late tertiary foreland basin evolution in the Timor Sea: constraints from foreland sequences, elastic flexure and normal faulting, Tectonophysics, 392, 37–54, https://doi.org/10.1016/j.tecto.2004.04.007, 2004.

Lüschen, E., Borrini, D., Gebrande, H., Lammerer, B., Millahn, K., Neubauer, F., and Nicolich, R.: TRANSALP — deep crustal Vibroseis and explosive seismic profiling in the Eastern Alps, Tectonophysics, 414(1–4), 9–38, https://doi.org/10.1016/j.tecto.2005.10.014, 2006.

Lüschen, E., Dussel, M., Thomas, R., and Schulz, R.: 3D seismic survey for geothermal exploration at Unterhaching, Munich, Germany, First Break, 29(1), 45–54, https://doi.org/10.3997/1365-2397.2011002, 2011.

Mallet, J.-L.: Geomodeling. Applied Geostatistics Series, Oxford University Press, New York, USA, 612 pp., 2002.

Marfurt, K. J.: Chapter 2, Seismic Attributes and What They Measure, in: Distinguished Instructor Series: Seismic Attributes as the Framework for Data Integration Throughout the Oilfield Life Cycle. SEG Books, 25–150, https://doi.org/10.1190/1.9781560803522.ch2, 2018.

Meyer, R. K. F., and Schmidt-Kaler, H.: Paläogeographischer Atlas des Süddeutschen Oberjura (Malm), E. Schweizerbart'sche Verlagsbuchhandlung, Stuttgart, 1990.

Moeck, I.: Catalog of geothermal play types based on geologic controls, Renewable and Sustainable Energy Reviews, 37, 867–882, https://doi.org/10.1016/j.rser.2014.05.032, 2014.

Mraz, E., Moeck, I., Bissman, S., and Hild, S.: Multiphase fossil normal faults as geothermal exploration targets in the Western Bavarian Molasse Basin: Case study Mauerstetten, Z. Dt. Ges. Geowiss., 169(3), 389–411, https://doi.org/10.1127/zdgg/2018/0166, 2018.

Müller, M.: Das Ergebnis der Bohrung Staffelsee 1 als Grundlage für neue Vorstellungen über Bau und Untergrund der gefalteten Molasse, Geologica Bavarica, 63, 86–106, 1970.

Müller, M.: Bohrung Miesbach 1: Ergebnisse der ersten im Rahmen des Erdgastiefenaufschlußprogramms der Bundesregierung mit offentlichen Mitteln geförderten Erdgastiefbohrung. Compendium, 75/76: 63–67, 1975/1976.

Müller, M., Nieberding, F., and Wanninger, A.: Tectonic style and pressure distribution at the northern margin of the Alps between Lake Constance and the River Inn, Geol. Rundsch., 77(3), 787–796, https://doi.org/10.1007/BF01830185, 1988.

Müller, M., and Nieberding, F.: Principles of abnormal pressures related to tectonic developments and their implication for drilling activities (Bavarian Alps, Germany), in: Oil and Gas in Alpidic Thrusbelts and Basins of Central and Eastern Europe, edited by: Wessely, G., and Liebl, W., EAGE Spec. Pub., 119–126, 1996.

Ortner, H., Aichholzer, S., Zerlauth, M., Pilser, R., and Fügenschuh, B.: Geometry, amount, and sequence of thrusting in the Subalpine Molasse of western Austria and southern Germany, European Alps, Tectonics, 34, 1–30, https://doi.org/10.1002/2014TC003550, 2015.

Paradigm Ltd.: SKUA-GOCAD, 2017.

Pfiffner, O. A.: Tectonic evolution of Europe — Alpine Orogeny, in: A Continent Revealed: The European Geotraverse, edited by: Blundell, D., Freeman, R., and Mueller, S., University Press Cambridge, Cambridge, U.K., 180–190, https://doi.org/10.1017/CBO9780511608261, 1992.

Price, N. J., and Cosgrove, J. W.: Analysis of geological structures, Cambridge University Press, Cambridge, 502 pp., 1990.

Reinecker, J., Tingay, M., Müller, B., and Heidbach, O.: Present-day stress orientation in the Molasse Basin, Tectonophysics, 482, 129–138, https://doi.org/10.1016/j.tecto.2009.07.021, 2010.

Roeder, D., and Bachmann, G.: Evolution, structure and petroleum geology of the German Molasse Basin, Mem. Mus. Natl. Hist. Nat., 170, 263–284, 1996

Schöpfer, M. P. J., Childs, C., and Walsh, J. J.: Location of normal faults in multilayer sequences, Journal of Structural Geology, 28, 816–833, https://doi.org/10.1016/j.jsg.2006.02.003, 2006.

Schulz, R., Thomas, R., Jung, R., and Schellschmidt, R.: Geoscientific prospect evaluation for the Unterhaching geothermal power plant, Z. Angew. Geol., 50(2), 28–36, 2004.

Scisciani, V., Tavarnelli, E., and Calamita, F.: Styles of tectonic inversion within syn-orogenic basins: examples from the Central Apennines, Italy, Terra Nova, 13, 321–326, https://doi.org/10.1046/j.1365-3121.2001.00352.x, 2001.

Sissingh, W.: Tectonostratigraphy of the North Alpine Foreland Basin: correlation of Tertiary depositional cycles and orogenic phases, Tectonophysics, 282, 223–256, https://doi.org/10.1016/S0040-1951(97)00221-7, 1997.

Schwerd, K., and R. Thomas, R.: Tektonische Strukturen am Alpennordrand bei Miesbach/Oberbayern in reflexionsseismischen Profilen — die Grenze zwischen Vorland und Faltenmolasse sowie die Basisüberschiebung von Helvetikum/Ultrahelvetikum und Rhenodanubischem Flysch, Zeitschr. Dt. Geol. Ges., 153, 187—207, 2003.

Tavani, S., Storti, F., Lacombe, O., Corradetti, A., Muñoze, J. A., and Mazzoli, S.: A review of deformation pattern templates in foreland basin systems and fold-and-thrust belts: Implications for the state of stress in the frontal regions of thrust wedges, Earth-Science Reviews, 141, 82–104, https://doi.org/10.1016/j.earscirev.2014.11.013, 2015.

Tavani, S., Corradetti, A., Sabbatino, M., Morsalnejad, D., and Mazzoli, S.: The Meso-Cenozoic fracture pattern of the Lurestan region, Iran: The role of rifting, convergence, and differential compaction in the development of pre-orogenic oblique fractures in the Zagros Belt, Tectonophysics, 749, 104–119, https://doi.org/10.1016/j.tecto.2018.10.031, 2018.

Tavarnelli E., and Peacock D. C. P.: From extension to contraction in syn-orogenic foredeep basins: the Contessa section, Umbria-Marche Apennines, Italy, Terra Nova, 11, 55–60, https://doi.org/10.1046/j.1365-3121.1999.00225.x, 1999.

Thomas, R., Schwerd, K., Bram, K., and Fertig, J.: Shallow high-resolution seismics and reprocessing of industry profiles in southern Bavaria: The Molasse and the northern Alpine front, Tectonophysics, 414, 87—96, https://doi.org/10.1016/j.tecto.2005.10.025, 2006.

Turcotte, D. L., and Schubert, G.: Geodynamics, J. Wiley and Sons, New York, 1982.

Tvedt, A. B. M., Rotevatn, A., Jackson, C. A.-L., Fossen, H., and Gawthorpe, R. L.: Growth of normal faults in multilayer sequences: A 3D seismic case study from the Egersund Basin, Norwegian North Sea, Journal of Structural Geology, 55, 1–20, https://doi.org/10.1016/j.jsg.2013.08.002, 2013.

Unger, H. J.: Die Lithozonen der Oberen Süßwassermolasse Südostbayerns und ihre vermutlichen zeitlichen Äquivalente gegen Westen und Osten, Geol. Bav., 94, 19–237, 1989.

von Guembel, C. W.: Geognostische Beschreibung des bayerischen Alpengebirges und seines Vorlandes, J. Perthes, 1, 1–440, 1861.

von Hagke, C., Lujiendjik, E., Ondrak, R., and Lindow, J.: Quantifying erosion rates in the Molasse basin using a high resolution data set and a new thermal model, Geotect. Res., 97, 94–97, https://doi.org/10.1127/1864-5658/2015-36, 2015.

von Hartmann, H., Tanner, D. C., and Schumacher, S.: Initiation and development of normal faults within the German alpine foreland basin: The inconspicuous role of basement structures, AGU Tectonics, 35, 1560–1574, https://doi.org/10.1002/2016TC004176, 2016.

Walsh, J. J., and Watterson, J.: Distributions of cumulative displacement and seismic slip on a single normal fault surface, Journal of Structural Geology, 9(8), 1039–1046, https://doi.org/10.1016/0191-8141(87)90012-5, 1987.

Walsh, J. J., Bailey, W. R., Childs, C., Nicol, A., and Bonson, C. G.: Formation of segmented normal faults: A 3-D perspective, Journal of Structural Geology, 25, 1251–1262, https://doi.org/10.1016/S0191-8141(02)00161-X, 2003.

Watterson, J.: Fault dimensions, displacements and growth, Pure and Applied Geophysics, 124, 365–373, https://doi.org/10.1007/BF00875732, 1986.

Weides, S., and Majorowicz, J.: Implications of spatial variability in heat flow for geothermal resource evaluation in large foreland basins: the case of the Western Canada Sedimentary Basin, Energies, 7(4), 2573–2594, https://doi.org/10.3390/en7042573, 2014.

Wibberley, C. A. J., Kurz, W., Imber, J., Holdsworth, R. E., and Collettini, C. (eds.): The Internal Structure of Fault Zones: Implications for Mechanical and Fluid-Flow Properties, Geol Soc. London Sp. Publ., 299, 2008.

Wilkins, S. J., and Gross, M. R.: Normal fault growth in layered rocks at Split Mountain, Utah: influence of mechanical stratigraphy on dip linkage, fault restriction and fault scaling, Journal of Structural Geology, 24(9), 1413–1429, https://doi.org/10.1016/S0191-8141(01)00154-7, 2002.

Withjack, M. O., Olson, J. E., and Peterson, E.: Experimental models of extensional forced folds, AAPG Bull., 74, 1038–1054, https://doi.org/10.1306/0C9B23FD-1710-11D7-8645000102C1865D, 1990.

Withjack, M. O., and Callaway, S.: Active normal faulting beneath a salt layer: an experimental study of deformation patterns in the cover sequence, AAPG Bull., 84(5), 627–651, https://doi.org/10.1306/C9EBCE73-1735-11D7-8645000102C1865D, 2000.

Ziegler, P. A.: Late Cretaceous and Cenozoic intraplate compressional deformations in the Alpine foreland — a geodynamic model, Tectonophysics, 137, 399–420, https://doi.org/10.1016/0040-1951(87)90330-1, 1987.

Ziegler, P. A.: Geological Atlas of Western and Central Europe, Shell Internationale Petroleum Maatschappij, B.V., The Hague, 1990.

Ziegler, P. A., Cloetingh, S., and van Wees, J.-D.: Dynamics of intra-plate compressional deformation: the Alpine foreland and other examples, Tectonophysics, 252, 7–59, https://doi.org/10.1016/0040-1951(95)00102-6, 1995.

Ziesch, J., Aruffo, C. M., Tanner, D. C., Beilecke, T., Dance, T., Henk, A., Weber, B., Tenthorey, E., Lippmann, A., and Krawczyk, C. M.: Geological structure of the CO2CRC Otway Project site, Australia: Fault kinematics based on quantitative 3D seismic interpretation, Basin Research, 29(2), 129–148, https://doi.org/10.1111/bre.12146, 2017.

Zweigel, J., Aigner, T., and Luterbacher, H.: Eustatic versus tectonic ~~control on foreland basin fill. Sequence stratigraphy , subsidence analysis , stratigraphic modelling, and reservoir modelling applied to the German Molasse Basin, Contr.Sedimen. Geol~~controls an Alpine foreland basin fill: Sequence stratigraphy and subsidence analysis in the SE German Molasse, ~~Stuttgart: E.Schweizerbart'sche Verlagsbuchhandlung,~~ in Cenozoic Foreland Basins of Western Europe, edited by A.Mascle, pp. 299—323, Geol. Soc., London., 299—323, 1998.

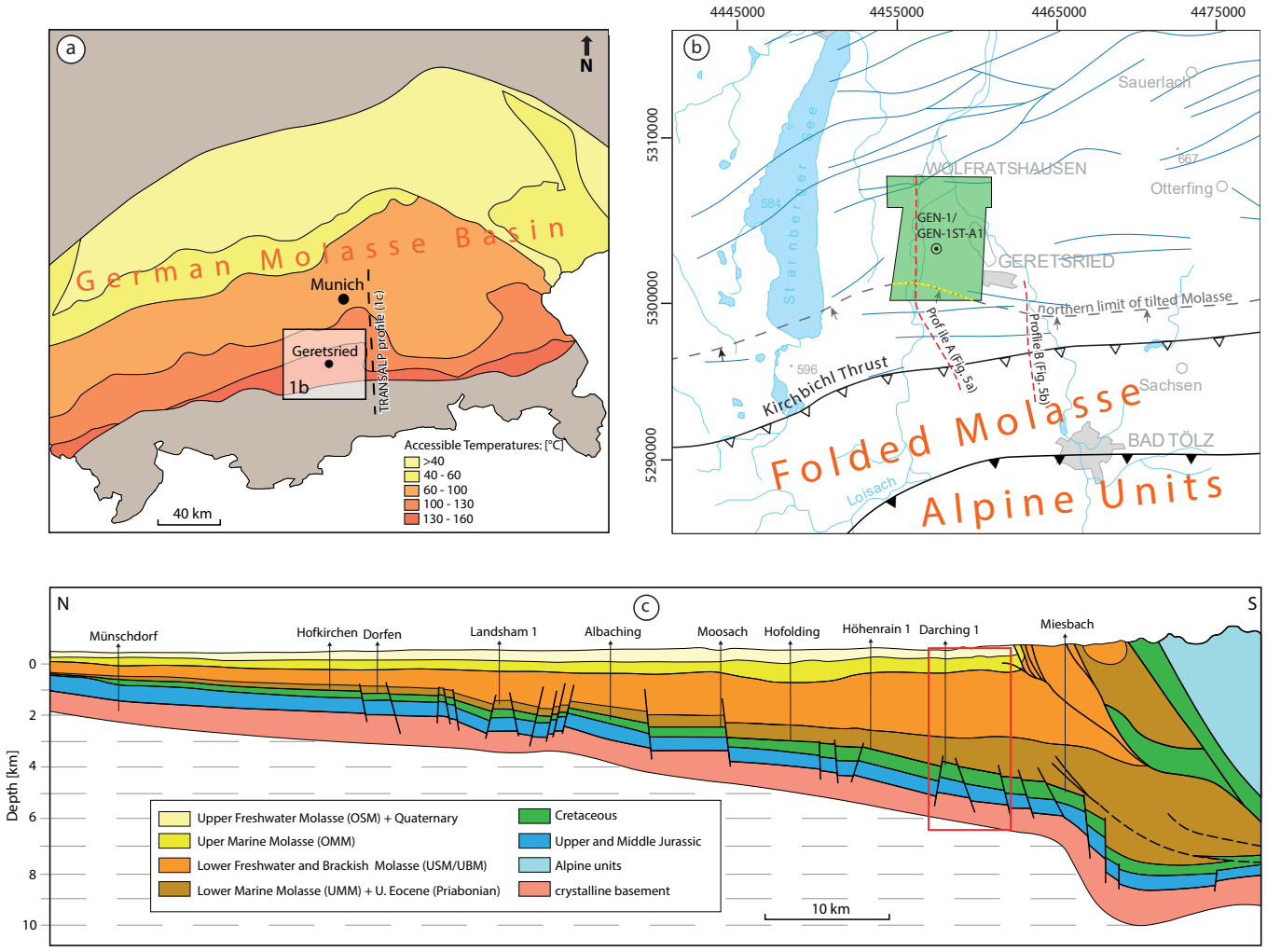

Figure 1. ~~Location map.~~ (a) Outline of the German Molasse Basin with geothermal areas (Agemar et al., 2014). Black box marks area shown in b. Black dashed line shows the location of the regional cross-section in ~~Figure 2~~1c. ~~Black box marks area shown in b.~~ (b) Close-up of the study area, showing the extent of the 3D seismic survey, the location of two seismic profiles and well GEN-1. Blue lines are traces of major normal faults in the Upper Jurassic carbonate platform (GeoMol Team, 2005). The dashed ~~yellow line shows the N extent of the Geretsried Fold. The dashed~~ grey line marks the N limit of the tilted Molasse according to the tectonic map of the Folded Molasse by Ortner et al. (2015)~~, whereas the dotted~~ . The dashed yellow line ~~is~~ shows the ~~interpretation of the~~ N ~~limit~~ extent of the ~~Folded Molasse based on this study~~Geretsried Fold. (c) Simplified cross-section across the Molasse Basin, based on the interpretation of the seismic TRANSALP profile (after Lüschen et al., 2006), located 30 km to the east of the study area. ~~For location, see Fig. 1a.~~ The red box marks the projection of the study area.

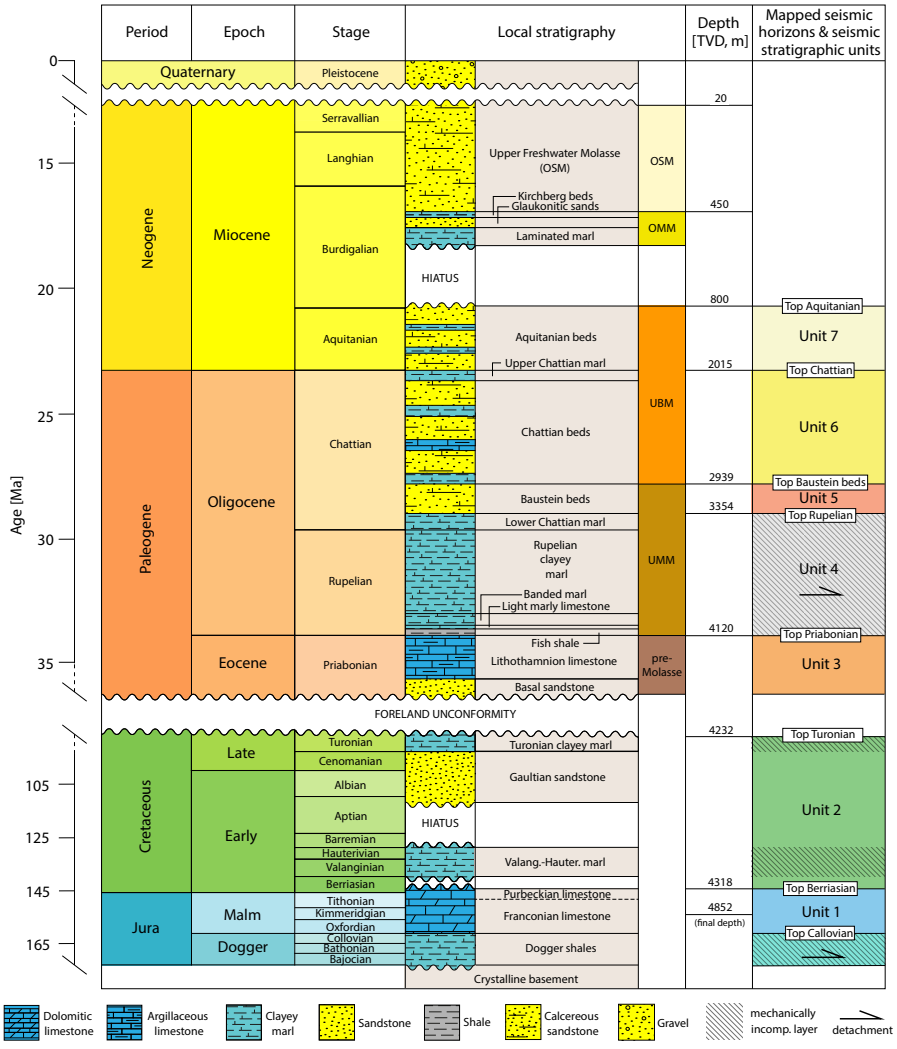

Figure 2. Detailed stratigraphy of the study area. Formation tops in depth were taken from the GEN–1 well. Qualitative mechanical stratigraphy (Fischer, 1960; Müller, 1970; Budach et al., 2017) and the location of inferred detachments (Bachmann et al., 1982; Müller et al., 1988; Ortner et al., 2015; von Hartmann et al., 2016) are also indicated. Mapped seismic horizons, and the stratal units they bound, are depicted in the right column. For stratigraphic abbreviations see Fig. ~~2~~1c.

a
b
c
d
N
S
Distance [km]
Depth b. m. s. l. [m]
upper fault array
lower fault array
U1
U2
U3
U4
U5
U6
U7
top Aquitanian
top Chattian
top Bausteine Bed
top Rupelian
top Priabonian
top Lutetian
top Bernasian
top Callovian
CZ Reverse F. 1
CZ Reverse F. 2
CZ Reverse F. 4
Upper Thrust
Geretsried Thrust
CZ normal faults
F. Gelting N
F. Gartenberg N
F. Gartenberg S
Fault NE

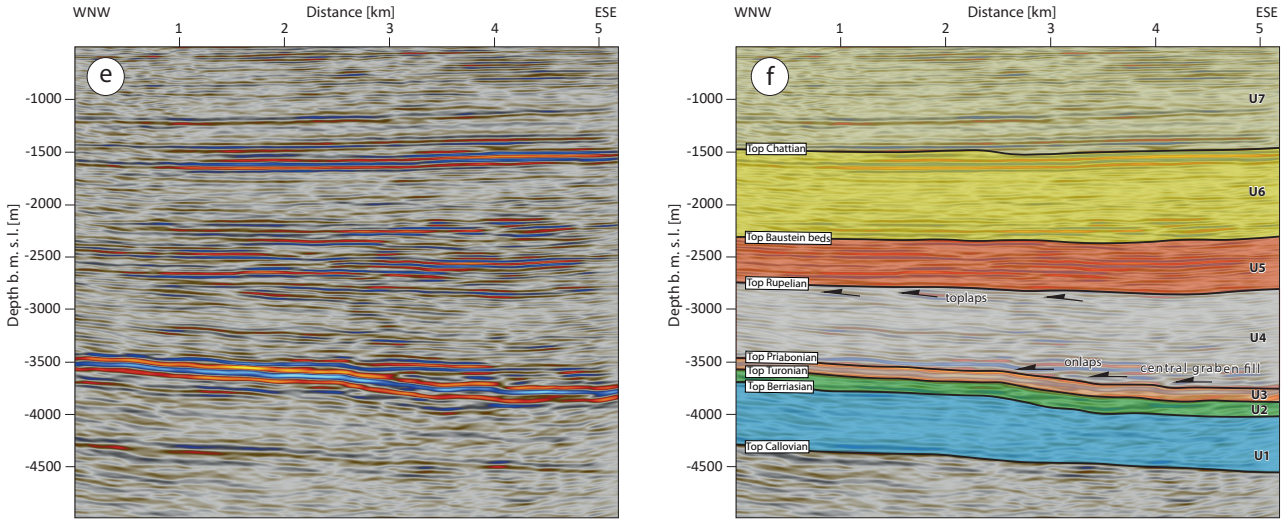

Figure 3. (a) N—S-oriented seismic section across the centre of the 3D survey, where (~~see Fig. 8 for location). (a) Depth section. (~~b) ~~Geoseismic section~~ is with interpreted seismic-stratigraphic units and faults~~, which illustrates that lower faults~~ . (c) and ~~upper faults are geometrically decoupled~~(d) N—S-oriented seismic section across the eastern margin of the 3D survey. The faults we refer to in this work are named. ~~WNW–ESE-oriented seismic section~~ (~~a~~e) ~~with interpretation~~ and (~~b~~f) WNW—ESE-oriented seismic section through the central graben, along its strike~~(see Fig~~. ~~8a for location).~~ It shows thinning of Unit 1 (carbonate platform), onlapping and toplapping of reflections within Unit 4. ~~N–S-oriented seismic section across the eastern margin of the 3D survey (see~~ See Fig. ~~8~~ 6 for location ~~)~~of the sections.~~(a) Depth section. (b) Geoseismic section with interpreted seismic-stratigraphic units and faults. The faults we refer to in this work are named.~~

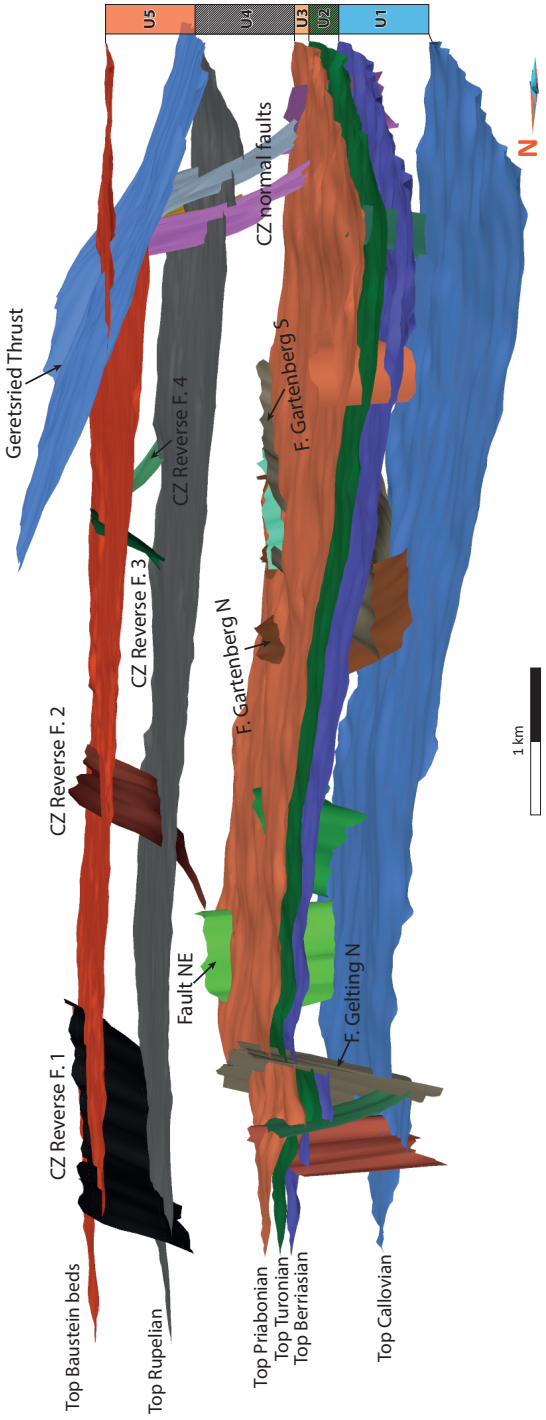

Figure 4. Oblique, WSW view of the 3D structural model showing two distinct fault arrays. The faults we refer to in this work are named.

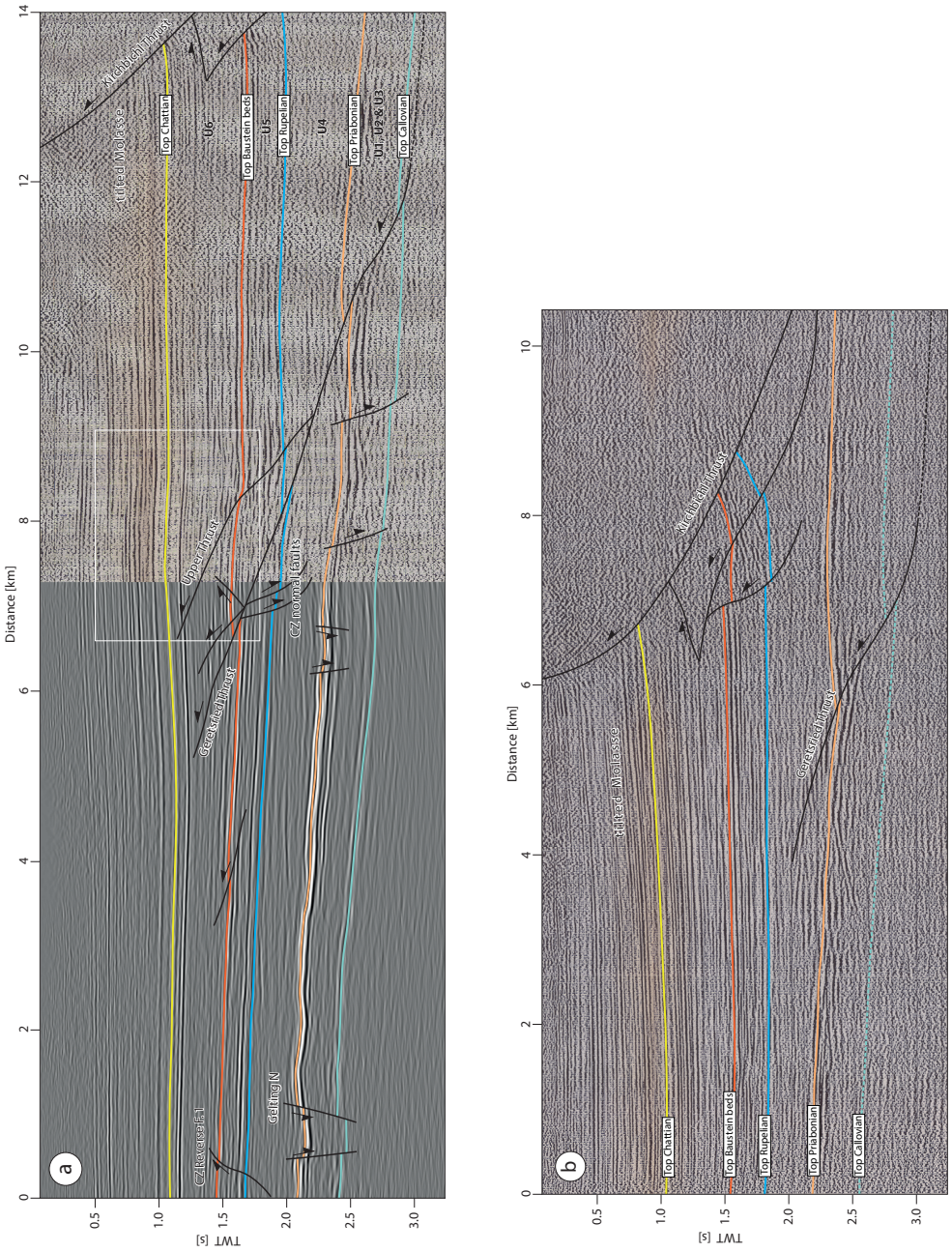

Figure 5. ~~Co-rendered variance and most negative curvature multiattribute maps and depth-structure maps, showing:~~ (a~~, b~~) ~~lower fault array at top Turonian, and (c, d) upper fault array at Top Rupelian and (e, f) at top Baustein beds.Isolines of the densities (> 1%) of the uniform distribution of poles to triangles that make up the surfaces of the lower faults, colour coded by fault. Lower hemisphere projection.N–S~~ N—S oriented seismic time profile A across the study area to the frontal thrust (i.e. ~~,~~Kirchbichl Thrust) of the Folded Molasse. It was produced by merging a cross-section from the 3D Geretsried seismic survey (left) and a 2D seismic line acquired in 1987 (right). The profile shows the extent and the cross-sectional geometry of the two major thrusts. The white box marks thrust-related folding within the hanging-wall of the Geretsried Thrust. For location ~~,~~of the profile A see ~~Fig~~Figures 1b and 6a—c, h. (b) N–S oriented seismic time profile B c. 3–5 km southeast of the Geretsried survey area. Note that the zone of tilted Molasse is much broader at this location. For location of the profile B see Figure 1b.

~~N–S oriented seismic time profile B, c. 3–5 km southeast of the Geretsried survey area. Note that the zone of tilted Molasse is much broader at this location. For location see~~

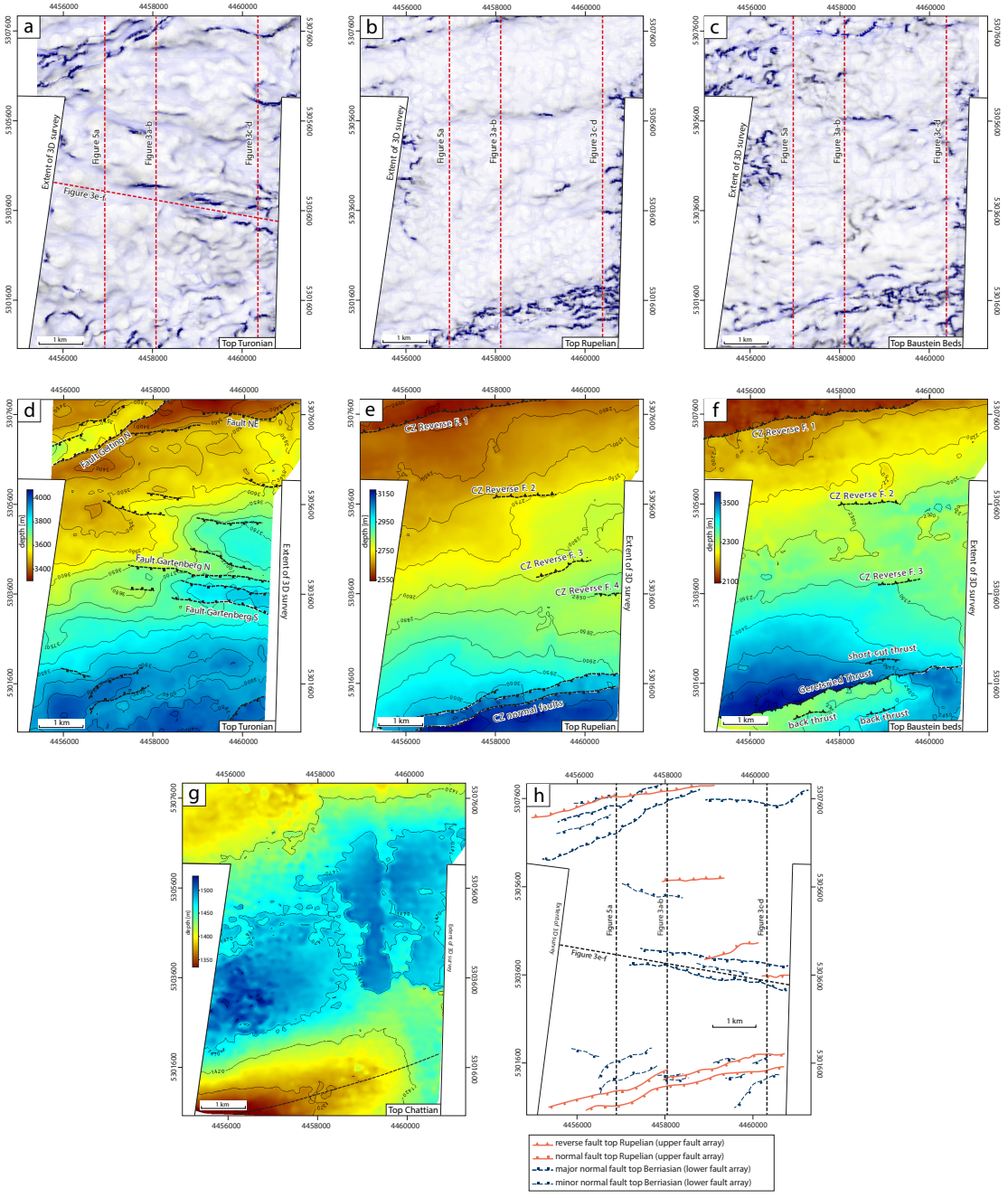

~~Figure 1b.~~

Figure 6. Co-rendered variance and most negative curvature multiattribute maps and depth-structure maps showing: (a), (d) lower fault array at top Turonian, (b), (e) upper fault array at Top Rupelian, and (c), (f) at top Baustein beds. (g) Depth-structure map of top Chattian showing termination of the Geretsried fold to ENE. Dashed line represents the fold hinge. (h) Map of fault traces interpreted within the 3D seismic volume.

~~Map of fault traces interpreted within the 3D seismic volume. Blue dashed lines are major and minor lower faults at top Berriasian, orange solid lines are upper faults at top Rupelian. The locations of the three cross-sections shown in Figures 4–6 and 10 are shown.~~

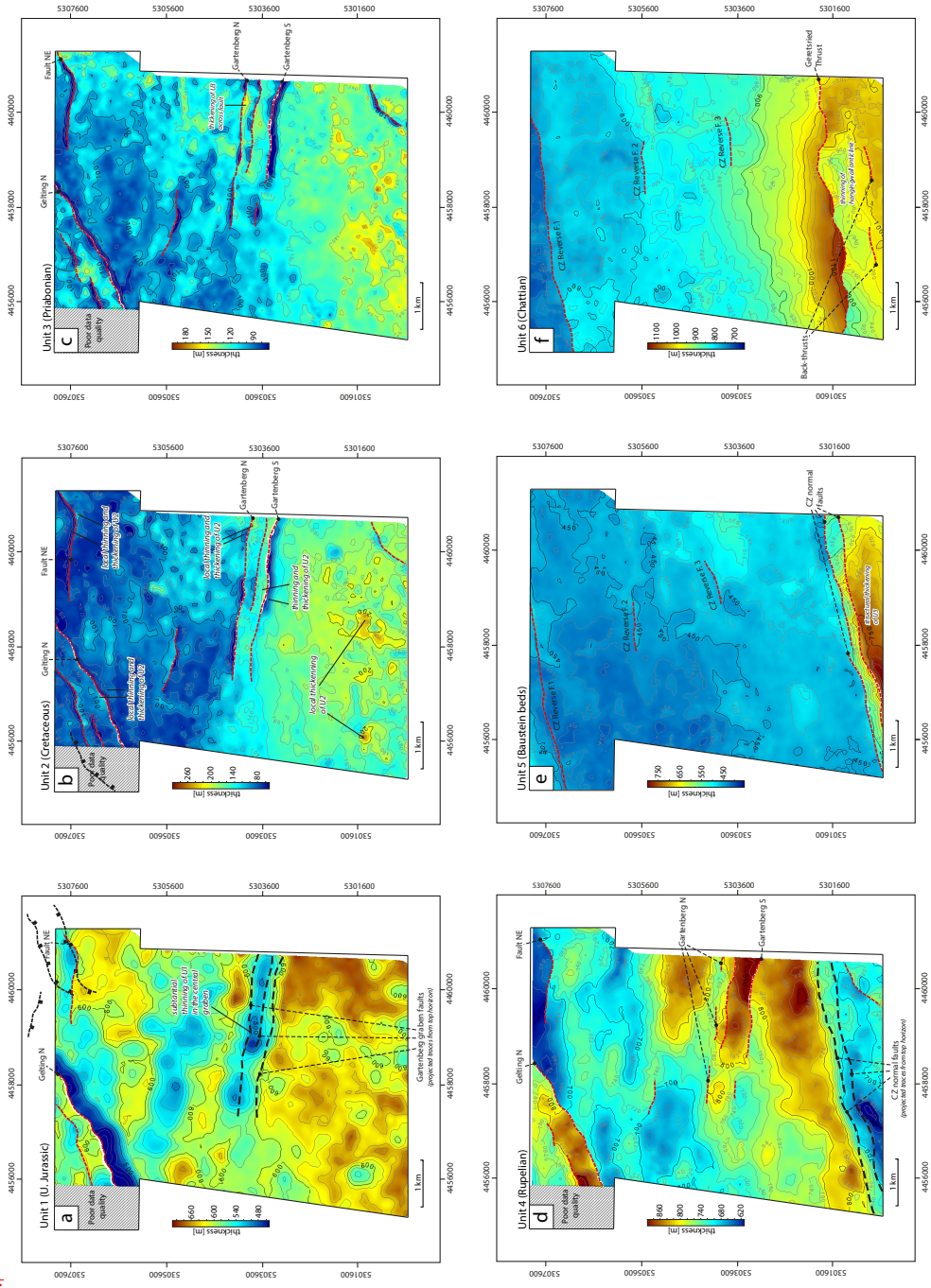

Figure 7. Isochore maps of the five stratigraphic units depicting sediment thickness changes and syn-kinematic growth strata. (a) Unit 1 (carbonate platform; Oxfordian to Early Berriasian); (b) Unit 2 (Valangian-Hauterivian marl, Gaultian sandstone, Turonian marl; Valangian to Turonian); (c) Unit 3 (Basal sandstone, Lithothamnion limestone; Priabonian); (d) Unit 4 (Rupelian clayey marls; Rupelian); Unit 5 (Baustein beds; Late Rupelian—Early Chattian); (f) Unit 6 (Chattian sandstones; Chattian). Note that the thickness minima on the footwall of the faults on thickness maps of Units 2 and 3 are not stratigraphic in origin, but are computational artefacts associated with the fault gap on top surface. See text for discussion.

~~Dip angle distribution on the Geretsried Thrust (map view). The black lines represent traces of the CZ normal faults juxtaposed by the Geretsried Thrust. Note that the step-over region between the CZ normal faults is characterised by higher dip~~

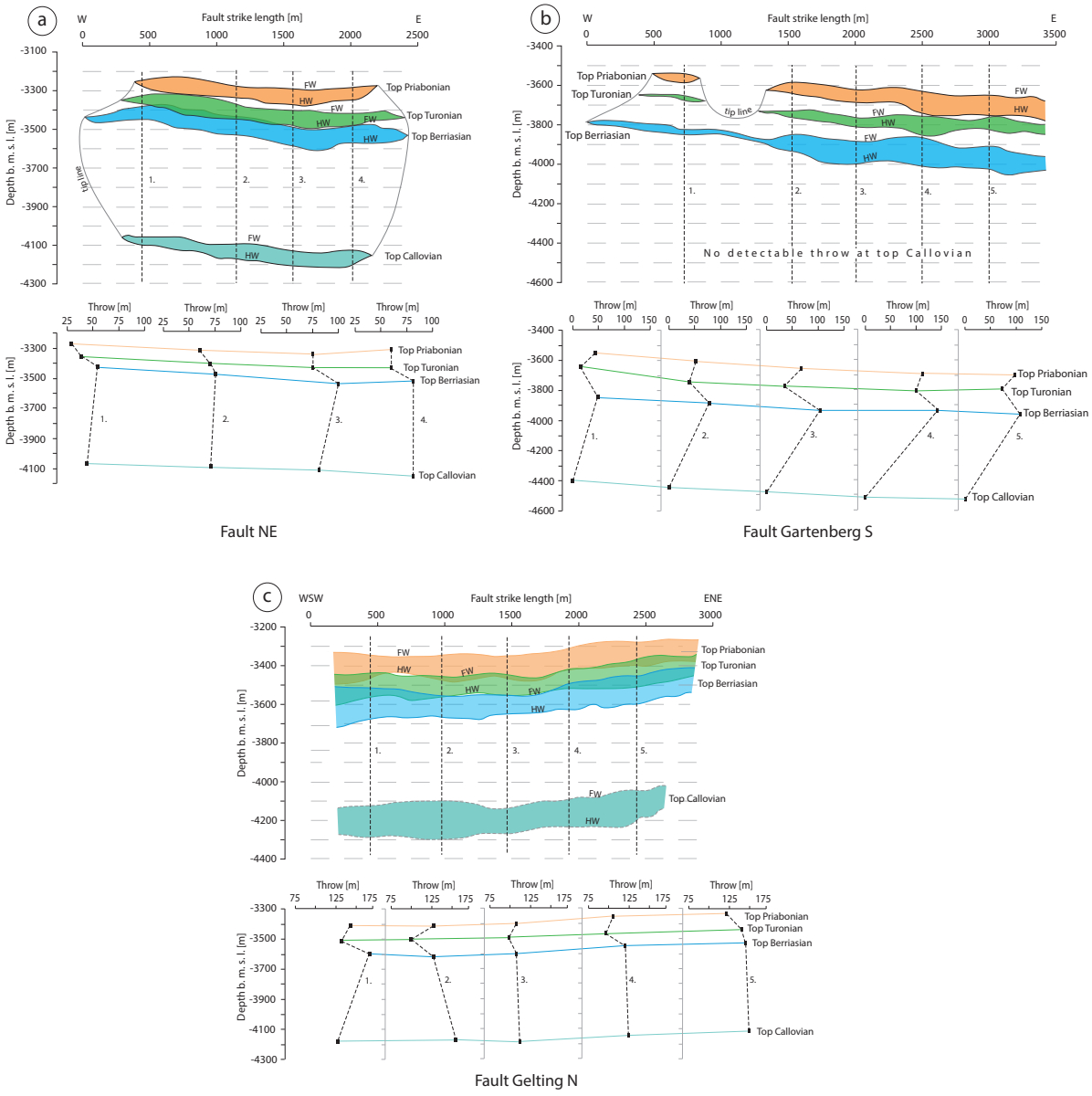

~~angle.~~

Figure 8. Allan maps and *t-z* plots for faults (a) NE, (b) Gartenberg S, and (c) Gelting N. Footwall and hanging-wall cut-offs are abbreviated FW and HW, respectively. (a) Fault NE: the throw decreases from top Berriasian stratigraphically upwards and downwards. The cut-offs of the horizons form a near-elliptical shape. (b) Fault Gartenberg S: the cut-off polygons show upward bifurcation of Fault Gartenberg S. Note throw reduction at top Turonian. (c) Fault Gelting N: the throw distribution shows no significant throw variations along the displaced horizons.

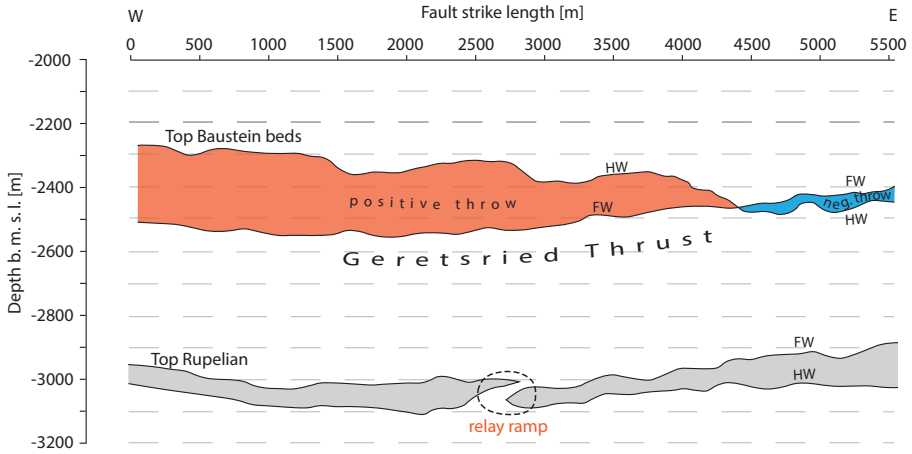

Figure 9. Alan map of the Geretsried Thrust at top Baustein beds (red for "positive" throw and blue for "negative" throw) and of the underlying normal faults at top Rupelian (grey). Note substantial decrease of throw on the Geretsried Lower Thrust to the E. See text for discussion. Footwall and hanging-wall cut-offs are abbreviated FW and HW, respectively.

~~Isochore maps of the five stratatigraphic units depicting sediment thickness changes and syn-kinematic growth strata. (a) Unit 1 (carbonate platform; Oxfordian to Early Berriasian); (b) Unit 2 (Valangian-Hauterivian marl, Gaultian sandstone, Turonian marl; Valangian to Turonian); (c) Unit 3 (Basal sandstone, Lithothamnion limestone; Priabonian); (d) Unit 4 (Rupelian clay; Rupelian); Unit 5 (Baustein beds; Late Rupelian–Early Chattian); (f) Unit 6 (Chattian sandstones; Chattian). Note that the thickness minima on the footwall of the faults on thickness maps of Units 2 and 3 are not stratigraphic in origin, but are computational artefacts associated with the fault gap on top surface. See text for discussion.~~

~~(a) Allan map and (b) *t*-*z* plot for Fault NE. Note that the throw decreases from top Berriasian stratigraphically upwards and downwards. The cut-offs of the horizons form a near-elliptical shape. Locations of *t*-*z* profiles are shown in a). Footwall and hanging-wall cut-offs are abbreviated FW and HW, respectively.(a) Allan map and (b) *t*-*z* plot for Fault Gartenberg S. The cut-off polygons show upward bifurcation of Fault Gartenberg S. Note throw reduction at top Turonian. Footwall and hanging-wall cut-offs are abbreviated FW and HW, respectively.(a) Allan map and (b) *t*-*z* plot for Fault Gelting N. The throw distribution shows no significant throw variations along the displaced horizons. Footwall and hanging-wall cut-offs are abbreviated FW and HW, respectively.Fault cut-off map of the Geretsried Thrust at top Baustein beds (red) and of the underlying normal faults at top Rupelian (grey). Note substantial decrease of throw on the Geretsried Lower Thrust to the E. See text for discussion. Footwall and hanging-wall cut-offs are abbreviated FW and HW, respectively.Depth-structure map of top Chattian showing termination of the Geretsried fold to ENE. Dashed line represents the fold hinge. No faulting occurs at this level.Stages of lower fault evolution based on the example of Fault NE: a) Nucleation of Fault NE within the carbonate platform; b) Up-dip propagation of the fault inhibited by multi-layered stratigraphy. Overlying units are forced to flex; c) Eventually, the fault breaches the monocline. The stagnant fault tip is buried by the later Rupelian sediments.~~

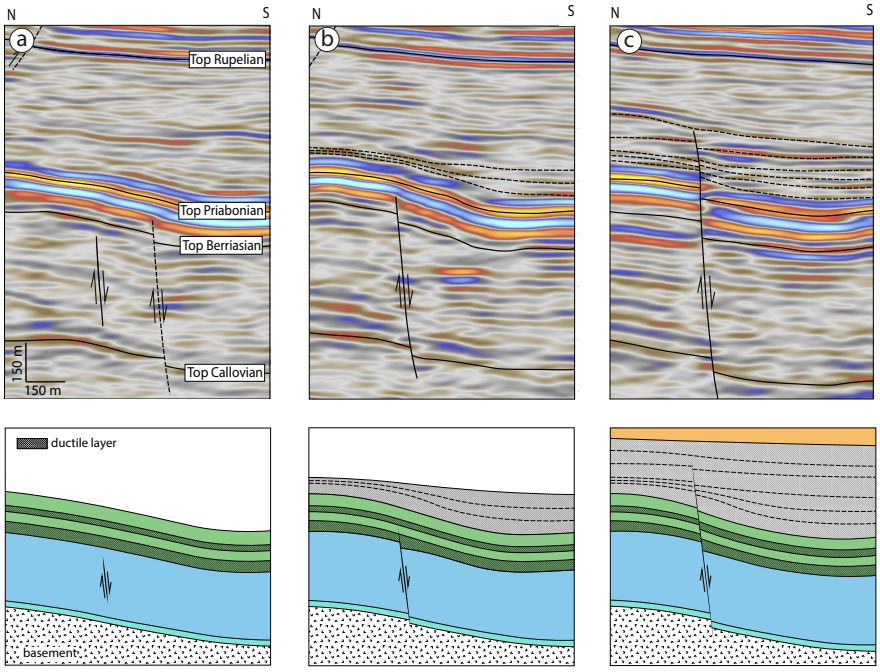

Figure 10. Stages of lower fault evolution based on the example of Fault NE: a) Nucleation of Fault NE within the carbonate platform; b) Up-dip propagation of the fault inhibited by multi-layered stratigraphy. Overlying units are forced to flex; c) Eventually, the fault breaches the monocline. The stagnant fault tip is buried by the later Rupelian sediments.